46th Annual Condensed Matter and Materials Meeting

Charles Sturt University, Wagga Wagga, NSW
6 to 9 February, 2024

CONFERENCE HANDBOOK

AUSTRALIAN INSTITUTE OF PHYSICS

46th Annual Condensed Matter and Materials Meeting

Charles Sturt University, Wagga Wagga, NSW
6 to 9 February, 2024

CONFERENCE HANDBOOK

2024 Organising Committee

Wayne Hutchison, UNSW Canberra (Chair)
Glen Stewart, UNSW Canberra
Oleh Klochan, UNSW Canberra
Daisy Wang, UNSW Sydney
Seán Cadogan, UNSW Canberra

CONTENTS

INTRODUCTION

The Annual Condensed Matter and Materials Conference, colloquially known as “Wagga”, has been held almost annually as a residential conference at the Charles Sturt University Conference Centre, Wagga Wagga, NSW, in February, since 1977. Unfortunately, due to the global pandemic known as COVID-19, the 45th Wagga conference had to be cancelled in 2021 and again in 2022. The series resumed in 2023. The Organising Committee is excited to welcome you to the 46th Annual Condensed Matter and Materials Meeting from Tuesday 6th to Friday 9th, February 2024. We are committed to providing a safe, in-person conference where we can catch up and hear about recent advances in Condensed Matter research from around Australia and New Zealand.

Diversity

Our aim is to facilitate an inclusive Meeting that encourages the free exchange of ideas and welcomes all voices in a respectful atmosphere. We invite participation from people of all races, ethnicities, genders, religions, nationalities, ages, sexual orientations and abilities.

As organisers, we are working to provide a balanced and diverse programme. The full Official Diversity and Equity Statement for the 46th Annual Condensed Matter and Materials Meeting 2024 can be found at https://www.aip.org.au/CMM-Conference.

WAGGA 2024 SPONSORS

Trade Booths: *Please visit these exhibitors who will be onsite throughout the conference.*

Gold Session Partner (Wednesday morning and Posters)

Child Care Bursaries and Student Prizes:

Satchel Insert:

MAPS

Wagga Wagga and the location of the Charles Sturt University campus

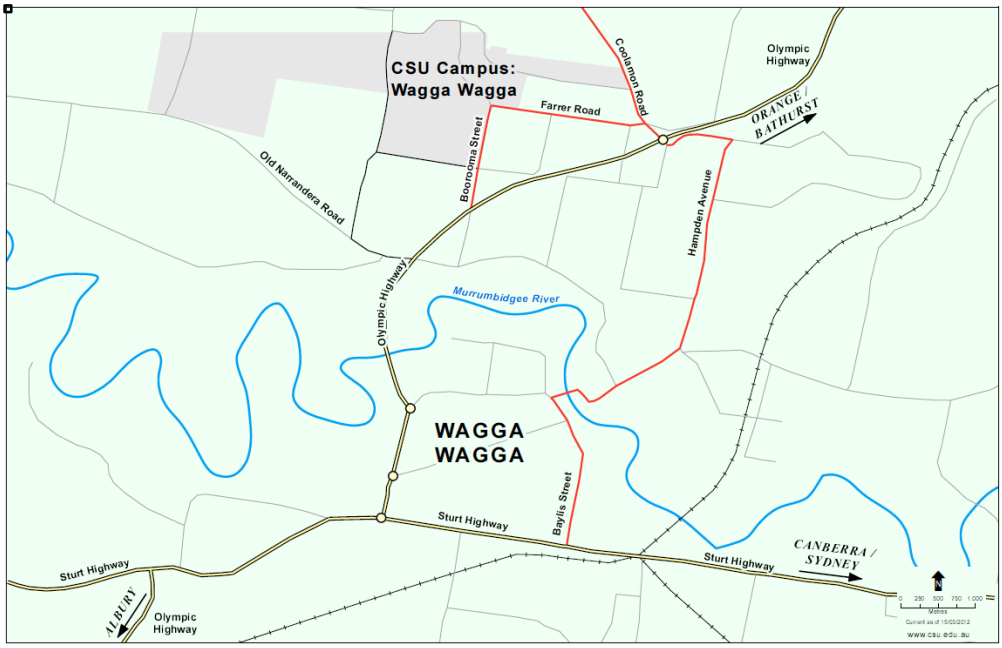

Location of Convention Centre and dormitory accommodation

Convention Centre and Dining Hall

Accommodation

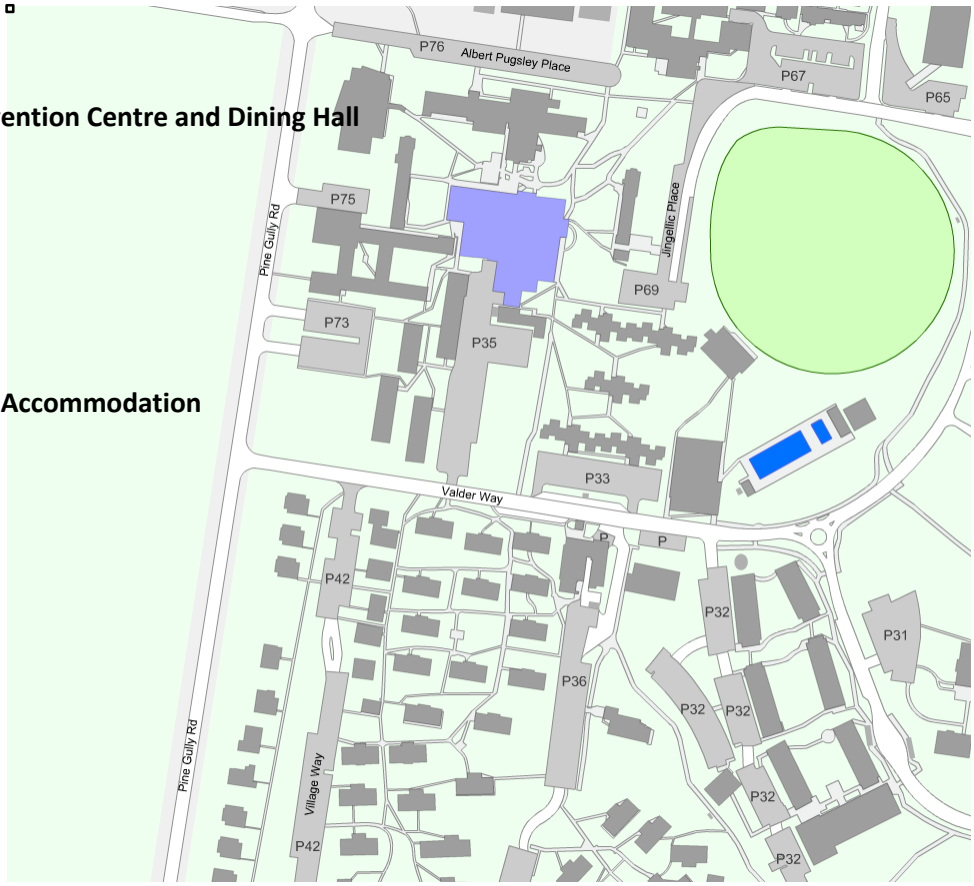

Location of Charles Sturt Winery and Cellar Door

The Tuesday evening wine tasting will now be held at the Cellar Door of the CSU Winery from 7.30 to 9.00 p.m. The map above shows the easiest walking path to the Winery from the Convention Centre. This should take about 20 minutes to walk or 4 minutes to drive.

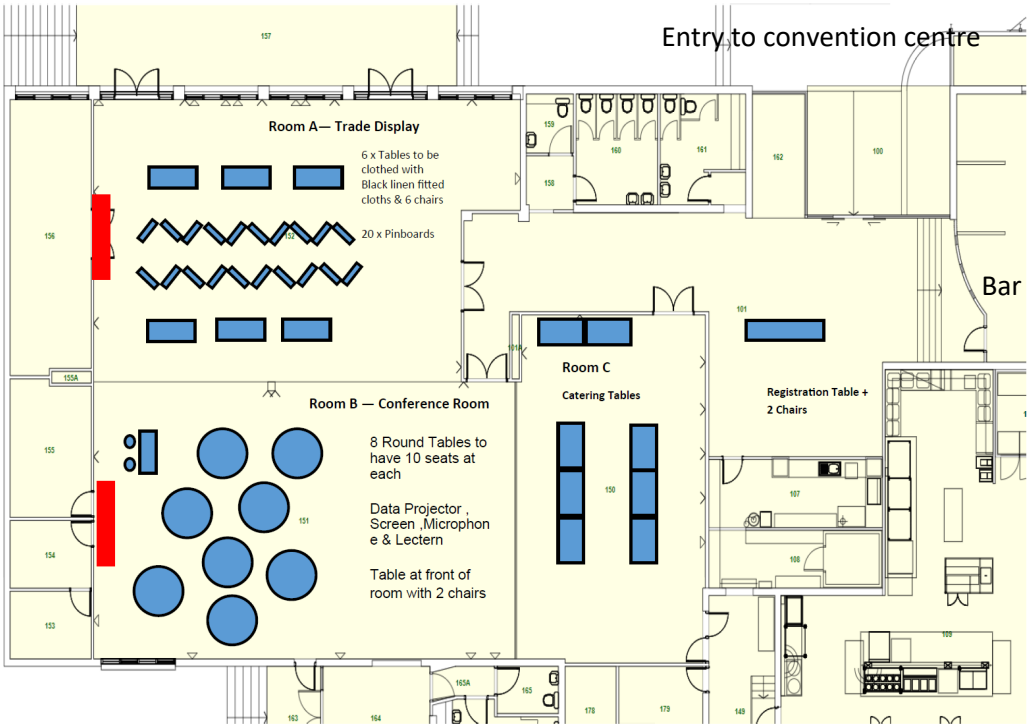

Layout of Convention Centre

THE CMM GROUP

Welcome to the “Wagga” community

Just by attending the annual Condensed Matter and Materials (CMM) Meeting you will join the mailing list of the CMM topical group of the Australian Institute of Physics (AIP). This way, you will hear updates about events such as the next Wagga conference via email. However, when you are renewing your AIP membership (or joining for the first time), please indicate your association with the CMM topical group by ticking the appropriate box. There are no additional forms or membership fees involved. If you do not wish to be part of this mailing list, please alert the conference organisers.

Take a look at the CMM Group web site

It can be accessed from the AIP national web site (www.aip.org.au) by clicking on “Branches & Groups” at the top of page and then selecting “Condensed Matter & Materials (CMM)”.

Alternatively, go directly to https://www.aip.org.au/Condensed-Matter-&-Materials-(CMM).

Please share your favourite “Wagga” experiences

If you have some special group images of you and colleagues, interesting events and stories from previous "Waggas", please share them with us by passing them on to Glen Stewart (g.stewart@adfa.edu.au) who will have them incorporated into a “Past Wagga Years, tributes” section of the CMM Group web site. Please include in your e-mail the year of the meeting and the names of those “Waggarites” you are able to identify in the images.

1978

2002

ATTENDEE INFORMATION

Scientific Programme:

All poster sessions and lectures will be held at the Convention Centre. Chairpersons and speakers are asked to adhere closely to the schedule for the oral programme. A PC laptop computer, pointer and microphone will be available. Please check that your presentation is compatible with the facilities provided as early as possible. Ideally, please load your presentation onto the central laptop in the break before your session. In particular, if you will be participating in the Poster Slam event before the poster sessions, your slides (**maximum** 2) must also be loaded onto the laptop during the lunch break. We encourage all Student Poster Presenters to participate in the Poster Slam. Posters should be mounted as early as possible. There will be numbers on each poster board corresponding to the place for your specific poster. Please check the programme for details. Please remove your posters by the close of the programme on Friday. There will be awards for the best Student Oral presentations and best Student Poster presentations and these awards will be presented on Friday before lunch.

Logistics:

Please wear your name-tag at all times. Registration and all other administrative matters should be addressed to the registration desk or a committee member. For lost keys or if you are locked out of your room, contact the Accommodation and Security Office near the corner of Valder Way and Park Way or phone them on 1800 931 633 (24 hrs).

Delegates must check out of their rooms on Friday morning, before 10:00am. All keys to be handed in at the registration desk in the convention centre.

Accommodation:

This year, “cottage” accommodation will be provided in Stewards Hall (building number 211), close to the Convention Centre:
https://www.csu.edu.au/current-students/uni-life/accommodation/wagga-wagga/stewards-halls
This includes private, single-bed rooms with shared bathroom facilities.
Ensuite accommodation will be provided in Hampden Village with private bathroom facilities:
https://www.csu.edu.au/current-students/uni-life/accommodation/wagga-wagga/hampden-village-undergraduate

Meals, Refreshments and Recreational Facilities:

Breakfast and Dinner will be served in the “Food Bowl” dining room at Atkins Hall, except the Conference Dinner on Wednesday 7th February, which will be held in the Convention Centre. Your name-tag and lanyard will serve as your dining room pass so please be sure to wear it to all meals. It may also be required as identification for use of all other campus facilities, which are at your disposal.

Lunch each day will be served in the Convention Centre. Morning and afternoon tea will be served in Room C of the Centre, as indicated in the timetable. In addition, on arrival on Tuesday afternoon from 4.00pm there will be a reception in the area near the food bowl, drinks will be from the Conference Bar. Wagga2024 will have a modest bar tab during the reception,

conference dinner and trivia night, but it is not limitless. At other times and whenever the tab limit is reached, you should expect to pay. This is a **cashless** bar, so please bring a credit card/phone to pay for drinks.

Good news (for those who recall last year), the swimming pool is open and delegates are able to use it so long as there is a lifeguard on duty. Pool Hours are 2 p.m. to 9 p.m.

The adjacent gymnasium and squash courts are open on weekdays from 6:00 a.m. until 9.00 p.m. A wide range of facilities such as exercise bikes, table tennis and basketball are available in the gymnasium. Access to these facilities is covered by your registration fee. Please bring your name-tag as proof of registration.

Wine Tasting evening:

Tuesday from 7:30 to 9:00 p.m. We will hold our wine tasting night at the Charles Sturt University Winery and Cellar Door. The location shown on the map on P6. This takes around 20 minutes to walk there. Please contact the conference organisers if you need assistance.

Convention Centre Contact Numbers:

Events Office Phone	(02) 6933 4910
After-hours Emergencies, Accommodation and Security	1800 931 633

Wireless Internet:

Available onsite through Eduroam. Eduroam covers 99% of buildings, outdoor areas and student residences. Alternatively, there is a guest net account. You will need to register for access to this, using the QR code which will be available throughout the Convention Centre and listed below. This registration only allows 48 hours access, so then please register again. See instructions or QR code on the next page.

Charles Sturt University

Connect to WiFi

Scan the below code to Connect to our Guest Wireless network

Or choose **CSU-Guest** from your device's wireless networks

> Select '**Click here to register for guest access**'
> Fill in the registration form
> Accept the Terms and Conditions and **Register**
> You will receive an SMS with your username and password
> Click **'Sign On'** to return to the login screen
> Enter your username and password
> Click **Accept** on the CSU Acceptable Use Policy

Your account will remain active for 48 hours

Division of Information Technology

TIMETABLE

Time	Tuesday Feb. 6	Wednesday Feb. 7	Thursday Feb. 8	Friday Feb. 9
7.30-8.45 a.m.		Breakfast	Breakfast	Breakfast
8.45 a.m.		Welcome: Wayne Hutchison		
		Chair: Tilo Söhnel	Chair: Amelia Liu	Chair: Stewart Campbell
9:00 a.m.		Kirrily Rule (*Invited*)	Matteo Baggioli (*Invited*)	Krystina Lamb (*Invited*)
9:15 a.m.				
9:30 a.m.		Shinichiro Yano	Amanuel Berhane	Mengting Zhao
9:45 a.m.		Dehong Yu	Caleb Stamper	Tanglaw Roman
10:00 a.m.		Sam Yick	Oliver Conquest	Mohammed Asiri
10:15 a.m.		Anton Stampfl	Huyen Pham	Kyle Portwin
10:30 a.m.		Morning tea	Morning tea	Morning tea
		Chair: Sue Coppersmith	Chair: Roger Lewis	Chair: Kirrily Rule
11:00 a.m.		Oleg Tretiakov (*Invited*)	Sue Coppersmith (*Invited*)	Xiaolin Wang (*Invited*)
11:15 a.m.				
11:30 a.m.		Eric Mascot	Daniel McEwen	Timothy Petersen
11:45 a.m.		Zeb Krix	Anindya Sundar Paul	Oscar Nieves
12:00 p.m.		Dmitry Efimkin	Dimi Culcer (*Invited*)	Jack Engdahl
12:15 p.m.		Feixiang Xiang		Awards and Closing
12:30 p.m.		Lunch	Lunch & CMM business	Lunch
		Chair: Krystina Lamb	Chair: Oleh Klochan	
2:00 p.m.	Registration from 2:00 pm	Tilo Söhnel (*Invited*)	David Pham (*Invited*)	
2:15 p.m.				
2:30 p.m.		Christopher Howard	Tours to Halocell	
2:45 p.m.		Jacob Martin		
3:00 p.m.		Klaus-Dieter Liss		
3:15 p.m.		Poster SLAM		
3:30 p.m.			Afternoon tea	
4:00 p.m.	Reception	Posters and	and posters	
5:00 p.m.	(Outside Food Bowl)	afternoon tea		
6:00 p.m.	Dinner		Dinner	
6:30 p.m.	(Food Bowl)	Conference dinner	(Food Bowl)	
7:30 p.m.	Wine Tasting (CSU Winery Cellar Door)	After dinner presentation: Evrim Yazgin (The Royal Institute)	Trivia night (Food Bowl)	
10:00 p.m.		(Convention Centre)		

LIST OF TALKS

W-1-1 Wednesday 09:00 Kirrily Rule (Invited), ANSTO
Taipan: a highly versatile neutron spectrometer for Condensed Matter investigations

W-1-2 Wednesday 09:30 Shinichiro Yano, NSRRC, Taiwan
Magnetic Phase Diagram of MnP

W-1-3 Wednesday 09:45 Dehong Yu, ANSTO
Single Particle to Collective Excitations –Mutual Cooperative Spin Coupling in Magnetic Materials

W-1-4 Wednesday 10:00 Sam Yick, University of Auckland
Controlling Skyrmions in Cu_2OSeO_3 through Doping; an insight to the relationship between crystal structure and magnetic ordering

W-1-5 Wednesday 10:15 Anton Stampfl, ANSTO
A semiempirical Hartree-Fock approach to solid-state calculations for inelastic neutron scattering

W-2-1 Wednesday 11:00 Oleg Tretiakov (Invited), University of New South Wales
Topotronics with Magnetic Topological Materials

W-2-2 Wednesday 11:30 Eric Mascot, University of Hamburg/University of Melbourne
Antiferromagnetism-driven Two-Dimensional Topological Nodal-Point Superconductivity

W-2-3 Wednesday 11:45 Zeb Krix, University of New South Wales
Non-Onsager Quantum Magnetic Oscillations

W-2-4 Wednesday 12:00 Dmitry Efimkin, Monash University
Weyl excitations via helicon-phonon mixing in conducting materials

W-2-5 Wednesday 12:15 Feixiang Xiang, University of New South Wales
Flat band engineering in Bernal-stacked Bilayer Graphene using Patterned Periodic Potential and Vertical Electric Field

W-3-1 Wednesday 14:00 Tilo Söhnel (Invited), University of Auckland
Synthesis and structural characterization of novel transition metal oxide clusters

W-3-2 Wednesday 14:30 Christopher Howard, University of Newcastle
Crystal Structures of the Tungsten Bronzes

W-3-3 Wednesday 14:45 Jacob Martin, Curtin University
Mechanism for graphite formation: experiments, simulations and virtual reality

W-3-4 Wednesday 15:00 Klaus-Dieter Liss, University of Wollongong
Grains ain't misbehaving or going wild? The initiation of abnormal grain growth!

T-1-1 Thursday 09:00 Matteo Baggioli (Invited), Shanghai Jiao Tong University
Who pulls the strings in amorphous systems? The stringlet theory of the boson peak

T-1-2 Thursday 09:30 Amanuel Berhane, CSIRO Manufacturing, Lindfield
The role of atomic and structural disorder in the critical voltage scaling of Al/AlOx/Al Josephson junction arrays

T-1-3 Thursday 09:45 Caleb Stamper, University of Wollongong
The Unique Lattice Dynamics of Nanodiamond – a Molecular Dynamics and Inelastic Neutron Scattering Investigation

T-1-4 Thursday 10:00 Oliver Conquest, University of Sydney
Supported 2D-Coordinated Networks for CO_2 Reduction: Role and Influence of the Substrate

T-1-5 Thursday 10:15 Huyen Pham, Monash University
Unraveling the local atomic order in the shear-bands of metallic glasses using scanning electron nano-diffraction

T-2-1 Thursday 11:00 Sue Coppersmith (Invited), University of New South Wales
Understanding and mitigating disorder effects in lithographically defined quantum nanodevices in semiconducting heterostructures

T-2-2 Thursday 11:30 Daniel McEwen, Monash University
Universal van der Waals Electrodes Technology for Two-Dimensional monolayer Semiconductors

T-2-3 Thursday 11:45 Anindya Sundar Paul, University of St. Andrews/Macquarie University
Local tuning of Rydberg exciton energies in nanofabricated Cu_2O pillars

T-2-4 Thursday 12:00 Dimi Culcer (Invited), University of New South Wales
Quantum kinetic theory of the orbital magnetic moment of Bloch electrons

T-3-1 Thursday 14:00 David Pham (Invited), Halocell Energy Ltd.
Metal Halide Perovskites for greener, more sustainable IoTs

F-1-1 Friday 09:00 Krystina Lamb (Invited), ANSTO
Updates on Project BRIGHT and a 4th Generation Synchrotron for Australasia

F-1-2 Friday 09:30 Mengting Zhao, Monash University & Australian Synchrotron
Realisation of epitaxial ultra-thin Kagome metal FeSn films

F-1-3 Friday 09:45 Tanglaw Roman, Flinders University
Simulating angle-resolved photoemission intensity maps

F-1-4 Friday 10:00 Mohammed Asiri, University of Adelaide
Protective ALD-Alumina Overlayer Prevents Agglomeration of Phosphine-Protected Au_9 Clusters on RF-TiO_2

F-1-5 Friday 10:15 Kyle Portwin, University of Wollongong
The phonon bandgap in thermoelectric SnSe: The role of dispersion interactions

F-2-1 Friday 11:00 Xiaolin Wang (Invited), University of Wollongong
Recent progress on new superconductors and superconducting electronic devices

F-2-2 Friday 11:30 Timothy Petersen, Monash University
Shape measurement by tracking topology in phase contrast and diffraction

F-2-3 Friday 11:45 Oscar Nieves, CSIRO Manufacturing, Lindfield
Theoretical Modelling of 2D SQUID Arrays

F-2-4 Friday 12:00 Jack Engdahl, University of New South Wales
Excitons in Atomically Thin TMD in Strong Magnetic Field

LIST OF POSTERS

(WEDNESDAY TO FRIDAY)

P1 Field-induced magnetic order of Sr_2RNbO_6 double perovskites, R = Ho, Er

Mustafa H. Ammar, Wayne Hutchison, Seán Cadogan and James Hester
The University of New South Wales, Canberra and ANSTO, Australia.

P2 Valence states, magnetic and transport anisotropy in a new room-temperature 2D vdW Ferromagnet: Fe_3GaTe_2

Mengyun You, Yong Fang, James Hester, Weiyao Zhao, Abduhakim Bake, Kirrily C Rule and Xiaolin Wang
University of Wollongong, Australia; Changshu Institute of Technology, People's Republic of China; ANSTO, Australia; Monash University, Australia.

P3 Does Iron have a Role in the Formation of Lightning Ridge Opals?

J D Cashion, B L Dickson, L P Aldridge and A Smallwood
Monash University; Gladesville NSW; Deakin University and International Opal Academy, Australia.

P4 Enhanced magnetocaloric effect accompanying successive magnetic transitions in $TbMn_2Si_{2-x}Ge_x$ compounds

H.Y. Hao, W.Q. Wang, W.D. Hutchison, J.Y. Li, C.W. Wang, Q.F. Gu, S.J. Campbell, Z.X. Cheng and J.L. Wang
Jilin University, Changchun, China; University of New South Wales, Canberra, Australia; National Synchrotron Radiation Research Centre, Taiwan; ANSTO, Australia; University of Wollongong, Australia

P5 Designing Multiferroic Heterostructures: A Density Functional Theory Study

F. Fakhera, O.J. Conquest, C. Verdi and C. Stampfl
University of Sydney and University of Queensland, Australia.

P6 Neutron diffraction study on Co-based melilite compounds

M. Kawamata, M. Avdeev and Y. Nambu
Tohoku University, Japan; ANSTO, Australia; Tohoku University, Japan; Japan Science and Technology Agency, Japan.

P7 Electronic structures and microstructures in $La_3Ni_2O_7$ superconductors

Kaiyu Ma, Abudulakim Bake, Joshua Maggiora, Rongkun Zheng, Zhi Li, Meng Wang, Weiyao Zhao and Xiaolin Wang
University of Wollongong; University of New South Wales, Sydney, NSW 2052 Australia; Sun Yat-Sen University, Guangzhou, China; Monash University, Australia

P8 Mössbauer Effect Examination of Fe in $RFe_2Sn_2Zn_{18}$ (R = Nd, Pr, La)
Wayne D. Hutchison, Glen A. Stewart, Seán Cadogan and Katsuhiko Nishimura
The University of New South Wales, Canberra, Australia and University of Toyama, Japan.

P9 Small-beam diffraction measurements for understanding local structure and local dynamics in glasses
A.C.Y. Liu, E. Bøjesen, S.T. Mudie, R.F. Tabor, A. Zaccone, P. Harrowell and T.P. Petersen
Monash University, Australia; Aarhus University, Denmark; ANSTO, Australia; University of Milan, Italy and University of Sydney, Australia.

P10 PELICAN –a Time of Flight Cold Neutron Spectrometer – Recent Scientific Outcomes and New Capabilities
Dehong Yu and Richard Mole
ANSTO, Australia

P11 Significant reduction of thermal conductivity of intermetallic Mg_2Si thermoelectric material from carbon fibre inclusion.
Md Rezoanur Rahman, Sheik Md Kazi Nazrul Islam, David Cortie, Caleb Stamper, Al Momin Md Tanveer Karim and Xiaolin Wang
University of Wollongong, CSIRO and ANSTO, Australia.

P12 Recent neutron polarisation analysis experiments at ACNS
Kirrily Rule, Nicolas de Souza, David Cortie, Andrew Manning and Shinichiro Yano
ANSTO, Australia, and National Synchrotron Radiation Research Centre, Taiwan.

P13 Removing Defect States from a Visible Light Photocatalytic Semiconductor for Solar Hydrogen using Atomic Layer Deposition of an Al_2O_3 Passivating Overlayer.
M. Smith and G. Andersson *Flinders University, Australia*

P14 DFT WIEN2k Generated Scattering Factors for lattice contraction studies employing QCBED in light metals
Andrew E. Smith, Tianyu Liu , Philip N.H. Nakashima, Laure Bourgeois , Z. Zhang
Monash University, Australia; University of Antwerp, Belgium and University of Oxford, UK.

P15 Terahertz Spectroscopy for Polyethylene Terephthalate (PET) Recycling
T. J. Sanders, J. L. Allen, J. Horvat and R. A. Lewis
University of Wollongong and ANSTO, Australia.

P16 Towards Observing Exciton-Polariton Rydberg Blockade in Cuprous Oxide
H. H. Vallabhapurapu, Anindya Sundar, Sai Kiran Rajendran, Hamid Ohadi and Thomas Volz
Macquarie University, Australia and University of St Andrews, UK

P17 Artificial bandstructure in GaAs lateral superlattices

D.Q. Wang, Z. Krix, C. Chen, D.A. Ritchie, O. Sushkov, A.R. Hamilton and O. Klochan

University of New South Wales, Sydney & Canberra; University of Cambridge, UK

INVITED TALKS

W-1-1 Taipan: a highly versatile neutron spectrometer for Condensed Matter investigations

K.C. Rule[a], M. You[b], K. Lord[c], K. Portwin[b] J. Allen[b] and W. Zhao[d]

[a] *Australian Centre for Neutron Scattering, ANSTO, NSW 2234, Australia.*
[b] *University of Wollongong, NSW, Australia.*
[c] *UNSW, Kensington, NSW, Australia.*
[d] *Monash University, Vic, Australia.*

Taipan is the thermal neutron spectrometer located in the reactor beam hall at the Australian Centre for Neutron Scattering. Originally built as a thermal Triple Axis Spectrometer (TAS), it has been part of the ACNS user program since 2010. Taipan has seen a number of major upgrades including the extension of the dance floor (2014), and the implementation of a new Cu-200 monochromator (2017) which allows Taipan to easily reach incident energies of 200meV [1]. Also, in 2017 a new secondary spectrometer, the Be-filter was installed allowing for rapid measurements of density of states of polycrystalline samples [2]. The TAS and Be-filter are interchangeable secondary spectrometers which are used at Taipan with a ratio of 75:25% respectively.

In this presentation, I would like to detail some recent results collected from Taipan with my students and early career researchers which highlight the versatility of this spectrometer for many different condensed matter investigations. Such results include work on low dimensional magnetic materials, magnetic thin films, thermoelectric materials, and magnetic coupling in amorphous materials. I would also like to present some recent Be-filter results on alanine, comparing these results to other spectroscopic measurements using alternate techniques.

[1] K.C. Rule *et al.*, *Nuclear Instruments and Methods in Physics Research A.* **901**, 140-149 (2018).
[2] G.N. Iles, K.C. Rule, V.K. Peterson, A.P.J.Stampfl and M.M. Elcombe, *Review of Scientific Instruments* **92**, 073304 (2021).

W-2-1 Topotronics with Magnetic Topological Materials

Oleg Tretiakov

School of Physics, University of New South Wales, 2052, NSW, Australia.

I will discuss topological magnetic textures, such as skyrmions, half-skyrmions (merons), bimerons and their anti-particles, which constitute tiny whirls in the magnetic order. They are promising candidates as information carriers for next generation electronics (thus called topotronics), as they can be efficiently propelled at very high velocities employing current-induced spin torques [1]. First, I will talk about skyrmions [2,3] and bimerons [4,5] in ferromagnetic systems coupled to heavy metals and topological materials. Then I will show that antiferromagnets can also host a variety of these textures, which have gained significant attention because of their potential for terahertz dynamics, deflection free motion [6], and improved size scaling due to the absence of stray field. Finally, I will demonstrate that topological spin textures, merons and antimerons, can be generated at room temperature and reversibly moved using electrical pulses in thin film CuMnAs, a semimetallic antiferromagnet that is a test-bed system for spintronic applications [7].

[1] B. Göbel, I. Mertig, and O. A. Tretiakov, *Phys. Rep.* **895**, 1 (2021).
[2] D. Kurebayashi and O. A. Tretiakov, *Phys. Rev. Research* **4**, 043105 (2022).
[3] M.-G. Han, ..., O. A. Tretiakov, et al., *Nano Lett.* **23**, 7143 (2023).
[4] B. Göbel, A. Mook, I. Mertig, and O. A. Tretiakov, *Phys. Rev. B* **99**, 060407(R) (2019).
[5] K. Ohara, ..., O. A. Tretiakov, et al., *Nano Lett.* **22**, 8559 (2022).
[6] J. Barker and O. A. Tretiakov, *Phys. Rev. Lett.* **116**, 147203 (2016).
[7] O. J. Amin, ..., O. A. Tretiakov, et al., *Nature Nano*. **18**, 849 (2023).

W-3-1 Synthesis and structural characterization of novel transition metal oxide clusters

M. S. Abdelbassit[a], S. Yick[a,b] and **T. Söhnel**[a,b]

[a] *School of Chemical Sciences, University of Auckland, Auckland 1142, New Zealand.*

[b] *MacDiarmid Institute for Advanced Materials and Nanotechnology, Wellington 6012, New Zealand*

A key structural feature across the stannate clusters is the formation of MSn_6-octahedra filled with different transition metals, forming either isolated or one-dimensional endless chains through shared corners and edges of the [MSn_6]-octahedra [1]. As the transition metal to tin ratio decreases, the coordination state of condensation increases systematically. Compounds like $RuSn_6[MO_4]O_4$ (M = Si, Al, Mn, Fe, Co, Zn, Mg), where [MSn_6]-octahedra do not condense, have been identified [1,2]. We have also reported new clusters of $Fe(Fe_{3-x}Mn_x)Si_2Sn_7O_{16}$ (x = 0…3) and $FeMn_3Ge_2Sn_7O_{16}$ which exhibit alternating octahedra of stannide and oxide layers as well as bridging units of SiO_4^{4-} and GeO_4^{4-} respectively [3,4].

A group of novel cluster compounds $Ir_3In_3Sn_{12}O_{14}$, $RuIn_6Sn_6O_{16}$ and $Ru_4In_2Sn_{20}O_{21}$ have recently been discovered, which exhibit new types of structures with proposed In^{+} and In^{+3} sites in addition to the possible oxidation states of Sn^{2+} and Sn^{1+}. Out of the three cluster compounds, only $RuIn_6Sn_6O_{16}$ contains highly ordered Sn/In sites with an alternating discrete $Ru(Sn)_6$ octahedra incapsulated in an indium oxide layer and additional substructure formed by indium occupying a site of sevenfold coordination. $Ru_4In_2Sn_{20}O_{21}$ show the formation of isolated and condensed clusters $RuSn_6$ clusters in the same compound for the first time. So far, only either isolated or condensed clusters could be found in a compound. $Ru_4In_2Sn_{20}O_{21}$ could be seen as a combination of $Ru_3Sn_{15}O_{14}$ and a (hypothetical) $RuSn_6[SnO_4]O_4$. $Ir_3In_3Sn_{12}O_{14}$ crystallizes in the $Ru_3Sn_{15}O_{14}$ structure type. The presentation will summarize the preparation and characterisation of these interesting novel materials.

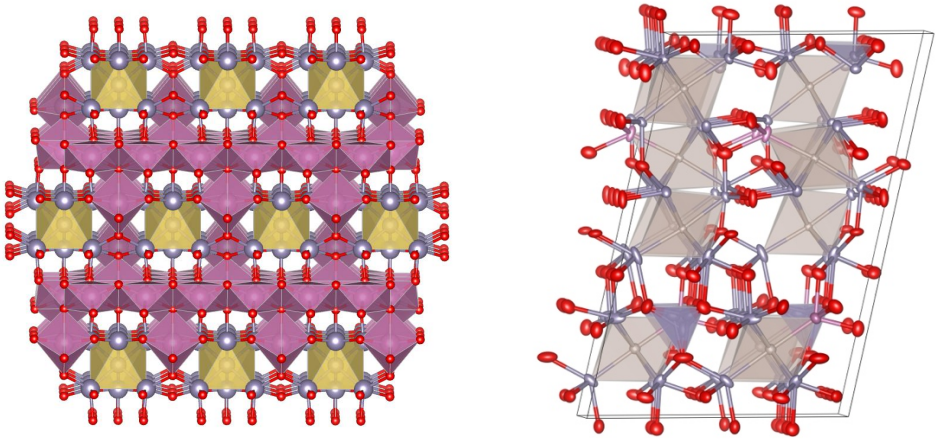

Figure 1. The crystal structure of $RuIn_6Sn_6O_{16}$ (left) exhibits discrete $Ru(Sn)_6$ octahedra (gold) and $In(O)_6$, $In(O)_7$ polyhedra (purple), and $Ru_4In2Sn_{20}O_{21}$ showing discrete and condensed $Ru(Sn)_6$ octahedra (right).

[1] Reichelt W., Söhnel T. *et al.*, *Angew. Chem. Int. Ed.* **34**, 2113 (1995); Söhnel, T., Reichelt, W., Wagner, F. E. Z. Anorg. *Allg. Chem.* **626**, 223 (2000).

[2] Söhnel, T. Z. Anorg. *Allg. Chem.* **634**, 2082 (2008).
[3] Söhnel T, Böttcher P, Reichelt W, Wagner F.E. Z. *Anorg. Allg. Chem.,* **624**, 708-714, (1998).
[4] Allison MC, Wurmehl S, Büchner B, Vella JL, Söhnel T, Bräuninger SA, Klauss HH, Avdeev M, Marlton FP, Schmid S, Ling CD. *Chem. Mater.* **34**, 1369 (2020).

T-1-1 Who pulls the strings in amorphous systems? The stringlet theory of the boson peak

Matteo Baggioli

Shanghai Jiao Tong University, China

The low-energy vibrational and thermal properties of crystalline solids can be successfully rationalized using Debye theory and the pivotal concept of phonons. Amorphous systems notably violate this paradigm. The most famous signature of this anomalous behavior is a low-frequency excess over the Debye level in the density of states, or equivalently in the low-temperature heat capacity, known as boson peak (BP). The microscopic origin of the BP is still subject of intense debate. Recently, Hu and Tanaka provided convincing simulation evidence that the BP might arise from quasi-localized 1D string-like excitations ("stringlets"), but a theory for that is still missing. In this talk, I will propose a simple model to explain the emergence of a BP anomaly from stringlet dynamics and show that its predictions are in beautiful agreement with the simulations by Hu and Tanaka. I will also discuss how the stringlet theory provides important insights on the temperature dependence of the density of states and the BP in the high-temperature liquid phase. Finally, I will comment about the emergence of glassy anomalies, including the BP, in crystalline systems with low or absent structural disorder and discuss possible explanations for it.

T-2-1 Understanding and mitigating disorder effects in lithographically defined quantum nanodevices in semiconducting heterostructures

Sue Coppersmith

School of Physics, UNSW Sydney

Making electronic nanodevices using semiconducting quantum well heterostructures is advantageous because the charge carriers are confined near a high-quality epitaxial interface that is relatively far from defects that degrade performance. This talk will discuss our work on optimising quantum devices in these heterostructures, which shows that is crucial to understand and control compositional disorder to optimise quantum dot qubits in Si/SiGe and that detailed electrostatic modelling yields new strategies for improving the properties of lithographically defined one-dimensional wires in GaAs/AlGaAs.

References:

B Paquelet Wuetz et al., Atomic fluctuations lifting the energy degeneracy in Si/SiGe quantum dots. *Nature Communications*, **13**(1), 7730 (2022).

T McJunkin et al., SiGe quantum wells with oscillating Ge concentrations for quantum dot qubits. *Nature Communications*, **13**(1), 7777 (2022).

MP Losert, et al., Practical strategies for enhancing the valley splitting in Si/SiGe quantum wells. *Physical Review B*, **108**(12), 125405 (2023).

K. Kumar et al., *B. Am. Phys. Soc*. F52.00010 (2023).

T-2-4 Quantum kinetic theory of the orbital magnetic moment of Bloch electrons

Dimi Culcer

School of Physics, UNSW, Sydney, NSW 2052, Australia

The orbital magnetic moment (OMM) of Bloch electrons has been known for a long time for over half a century, and a well established semiclassical description of it exists. It has come under renewed scrutiny recently as part of a general effort to understand angular momentum dynamics in systems in which spin-orbit interactions are absent or negligible - including graphene, transition metal dichalcogenides, and topological antiferromagnets. Yet despite intense interest in the OMM its fundamental properties are poorly understood. At present there is no quantum mechanical theory of the OMM, part of the problem being that dealing with the position operator between Bloch states is non-trivial. This is a significant gap: without knowing when the OMM is conserved, for example, we cannot discuss meaningfully orbital currents and the orbital Hall effect.

I will present two recent results from our group. The first is related to the orbital Hall effect. The theory of the orbital Hall effect (OHE), a transverse flow of orbital angular momentum in response to an electric field, has concentrated overwhelmingly on intrinsic mechanisms. We have determined the full OHE in the presence of short-range disorder using 2D massive Dirac fermions as a prototype. We find that, in doped systems, extrinsic effects associated with the Fermi surface (skew scattering and side jump) provide ≈95% of the OHE. This suggests that, at experimentally relevant transport densities, the OHE is primarily extrinsic.

In the second part I will introduce a quantum mechanical theory of the OMM due to intrinsic mechanisms. The theory is based on the density matrix and quantum Liouville equation. I will show that the OMM is in general not conserved in an electric field. The force moment produces a torque on the OMM, which is determined by the quantum geometric tensor and the group velocities of Bloch bands. The torque vanishes in two-band systems with particle-hole symmetry but is nonzero otherwise. For tilted massive Dirac fermions the torque is determined by the magnitude and direction of the tilt.

T-3-1 Metal Halide Perovskites for Greener, more Sustainable IoTs

David Pham

Halocell Energy Ltd., 286 Byrnes Road, Bomen, NSW 2650, PO Box 5033

The rapid development of the Internet of Things (IoTs), ranging from smart home appliances to industrial sensors has catalysed an unprecedented demand for reliable, energy-efficient solutions, particularly in indoor environments where conventional power sources may be constrained. Metal halide perovskites, known for remarkable opto-electronic properties, tunable bandgap, and ease of fabrication, have emerged as promising candidates for low-cost, high-efficiency indoor photovoltaics. In this talk, I will firstly illustrate our findings on the theoretical maximum efficiencies versus band gap measured for indoor photovoltaic devices under LED light. Specifically, the ideal bandgap for such LED light sources is in the range of 1.7-1.9 eV, with a maximum efficiency of 55% achieved at a bandgap of 1.74 eV. Then, I will demonstrate our recent strategy of using guanidium bromine to reduce non-radiative losses associated with wide bandgap perovskites and their interfaces, enabling the 1.74 eV-perovskite solar cell/module to achieve efficiency of 38.4%/29.9%, respectively, under weak indoor light (warm LED, 1000 lux). Finally, I will discuss Halocell's recent development on roll-to-roll production of perovskite solar module for indoor IoT applications.

F-1-1 Updates on Project BRIGHT and a 4th Generation Synchrotron for Australasia

K. E. Lamb, P. Kappen

Australian Synchrotron, ANSTO

The Australian Synchrotron at ANSTO has been delivering strong science outcomes since it opened its doors in 2007. The current BRIGHT Program, increasing the facility's capabilities from 10 to 18 beamlines, is an important part of continuing to support cutting edge research for the user community. Once complete, the full suite of beamlines will operate across six groups of methods: Crystallography, Imaging, Diffraction, Scattering, Microscopy, and Spectroscopy. We also expect that the Australian Synchrotron will reach an end of life by the late 2030s, by which time science drivers will demand more than the current facility can technologically deliver regardless of further upgrades. Synchrotron science and technology will have moved on significantly, and several 4th generation synchrotrons will have materialised around the world. It is thus time to think about how we could move to next generation synchrotron science in Australia and our region.

In this contribution, we will discuss first results and outputs of the new BRIGHT beamlines as well as other upgrade opportunities around the original beamlines. We will discuss the updates to the MCT, MEX1, MEX2 and BioSAXS user program, and then the current progress of the MX3, Nanoprobe, ADS1 and ADS2 beamlines. We will then discuss a few highlight projects that are upgrading the original capabilities, including the SXR, XAS and XFM capabilities.

We will also explore science and technology parameters for a new synchrotron lightsource. As next generation synchrotrons deliver significantly higher brightness and better photon beam coherence than our current facility, giving us access to time-resolved measurements at the millisecond scale, microscopy at low- or sub-nm resolution, and more.

This presentation seeks to showcase the recent and near future development at the Australian Synchrotron and to drive a dialogue with the broader community and solicit input into plans and proposals for a 4th generation synchrotron for Australasia.

F-2-1 Recent progress on new superconductors and superconducting electronic devices

Xiaolin Wang[a,b]

[a]*Institute for Superconducting and Electronic Materials, Australian Institute for Innovative Materials, University of Wollongong, Fairy Meadow, Australia*
[b]*Australian Research Council Centre of Excellence in Future Low Energy Electronics Technologies, University of Wollongong, Australia*

Email: xiaolin@uow.edu.au

In recent years, there has been rapid progress in the field of superconductors and superconducting electronics. I will provide an overview of the recent significant advancements, including the discovery of new types of superconductors, such as 2D superconductors, topological superconductors, high-entropy superconductors, and a new class of Ni-based superconductors with T_c above 77K [1,2]. Additionally, I will discuss enhancements in T_c and J_c achieved through pressure or gating effects [3,4]. Furthermore, I will delve into the recent discovery of superconducting diode effects [5], which hold great potential for the development of novel superconducting electronics technology.

1. Hualei Sun et al., *Nature*, **621**, 493 (2023).
2. [Review] Lina Sang, Zhi Li, Guangsai Yang, Muhammad Nadeem, Lan Wang, Qikun Xue, Alexander R. Hamilton and Xiaolin Wang, *Matter*, **5**, 1734-1759 (2022).
3. [Review] Lina Sang et al., *Materials Physics Today*, **19**, 100414 (2021).
4. [Review] P Liu, Bin Lei, Xianhui Chen, Lan Wang and Xiaolin Wang, *Nature Reviews Physics* **4**, 336 (2022).
5. [Review] Muhammad Nadeem, Michael S. Fuhrer and Xiaolin Wang, *Nature Reviews Physics,* **5**, 558 (2023).

CONTRIBUTED TALKS

W-1-2 Magnetic Phase Diagram of MnP

Shinichiro Yano

National Synchrotron Radiation Research Centre, Hsinchu, Taiwan.

Manganese phosphide MnP has been investigated for decades because of its rich magnetic phase diagram [1,2]. It has a slightly distorted NiAs structure with the space group *Pbnm* (No.62) with lattice parameters a = 5.91 Å, b = 5.25 Å, and c = 3.18 Å. The magnetic structure of MnP is ferromagnetic below T_C = 291 K and helimagnetic structure at T_S = 47 K with a propagation vector k = 0.117 a*. The phase diagram of the *H-T* shows a special tricritical point which is the point where the ferro-fan-paramagnetic phases meet. This is known as the Lifshitz point. MnP is the first magnetic system in which the Lifshitz point has been established to exist. In addition to this, the discovery of superconductivity in MnP was reported under pressures of 8 GPa and with T_{SC} around 1 K [3]. This makes MnP the first Mn-based superconductor. After the discovery, several studies from X-ray and neutron scattering under pressure have been performed [4,5,6]. Although there are several discrepancies, the results completed the *P-T* phase diagram of MnP, which revealed new magnetic phases before the system reaches the superconducting phase. These two *H-T* and *P-T* phase diagrams of MnP are quite interesting.

By using single crystals and a number of neutron inelastic scattering instruments, we have completed observation magnetic excitation of MnP at ambient pressure at helical and ferromagnetic phases. The spin Hamiltonian and exchange parameters of MnP are determined.

$$H = \sum_{mi,mj} J_{mi,mj}\, \boldsymbol{S_i} \cdot \boldsymbol{S_j}$$

Here m and n are the unit cell, i and j are sublattice in the unit cell. The exchange parameters determined at the ferromagnetic phase are J_1 = 22.78 meV, J_2 = 45.62 meV and J_4 = –5.26 meV at 60K. We simply define the parameter J_n as the exchange parameters of the n-th nearest neighbour of Mn-Mn. So, the ratios are R=J_1/J_2 = 2 and R'= J_4/J_2 = -0.23, which are consistent with an estimation based on the DFT calculation by Xu *et al* [7]. I will discuss the relation between these determined parameters and the phase diagram of MnP in this talk.

[1] Neutron scattering from magnetic materials; Tapan Chatterji.
[2] Andrzej. Zieba, Monika Slota and Mariusz Kucharcyk, *Phys. Rev. B* **61** 3435 (2000).
[3] J.-G. Cheng, K. Matsubayashi, W. Wu, J. P. Sun, F. K. Lin, J. L. Luo and Y Uwatoko, *Phys. Rev. Lett*, **114** 117001 (2015).
[4] Yishu Wang, Yejun Feng, J.-G. Cheng, W. Wu, J. L. Luo and T. F. Rosenbaum, *Nat. Commun*., **7** 13037 (2016)
[5] Shin-ichiro Yano, Diane Lançon, Henrik M. Rønnow, Thomas C. Hansen, Eric Ressouche, Navid Qureshi, Bachir Ouladdiaf and Jason S. Gardner, *J. Phys. Soc. Jpn*. **87** 023703 33-38 (2018)
[6] M. Matsuda, F. Ye, S. E. Dissanayake, J.-G. Cheng, S. Chi, J. Ma, H. D. Zhou, J.-Q. Yan, S. Kasamatsu, O. Sugino, T. Kato, K. Matsubayashi, T. Okada and Y. Uwatoko, *Phys. Rev. B* **93**, 100405(R) (2016).
[7] Yuanji Xu, Min Liu, Ping Zheng, Xiangrong Chen, Jin-guang Cheng, Jianlin Luo, Wenhui Xie and Yi-feng Yang; *J. Phys.: Condens. Matter* **29** 244001 (2017).

W-1-3 Single Particle to Collective Excitations –Mutual Cooperative

Spin Coupling in Magnetic Materials

Narendirakumar Narayanan[a,b], Richard Mole[a] and Dehong Yu[a]

[a]*Australian Centre for Neutron Scattering, Australian Nuclear Science and Technology Organisation, New Illawarra Road, Lucas Heights, 2234, Australia.*

[b]*Research School of Chemistry, The Australian National University, ACT 2601, Australia.*

Rare-earth orthoferrites RFeO$_3$ (R = rare earth), as a series of classical magnets, have been actively investigated for decades due to that many novel properties are continually being discovered and bringing surprise to us. These include, but it is not limited to, the high temperature multiferroic properties of BiFeO$_3$ [1] and the ultrafast spin manipulation in the THz regime on DyFeO$_3$, ErFeO$_3$ and NdFeO$_3$, [2]. These discoveries offer promising applications in many technical areas such as wireless communication, optomagnetic memory, quantum computing and spintronics. Thus, fundamental understanding of the magnetic properties of rare earth orthoferrites becomes essential to realize the application potentials of these materials.

Here we report a direct observation of cooperative magnetic interaction between two sublattices in the classic orthoferrite, PrFeO$_3$, using inelastic neutron scattering. The experiment reveals the transition from single particle excitation (crystal field excitation) to collective excitation (spin wave like excitation) of Pr^{3+} ions as a function of temperature. Theoretical modelling with DFT, linear spin wave theory (LSWT) and dynamical susceptibility calculation based on Random Phase Approximation (RPA-McPhase) reproduce the experimental observations and extract various exchange couplings. At low temperature, the Pr^{3+} can be considered as a quasi-two-level system because of exchange interaction due to the ordered Fe spin system. The spin wave associated with the canted ferromagnetic moments polarizes the Pr moment through Fe-Pr interaction, which in turn enhances the Pr-Pr coupling. With decreasing temperature, these interactions become more important and changes the crystal field excitation to an emergent spin wave like excitation, accompanied with the magnetic phase transition of the Fe subsystem. The intrinsic ferromagnetic component of Fe on the other hand induces a mode splitting and mimics the effects of an external magnetic field on the dispersive magnetic excitations of Pr. The study indicates that, at atomic level, the nature of cooperative interaction between sub-systems is intrinsic, general, and mutual if the energy scale is match.

[1] J. Wang, *et al*. *Science* **299**, 1719 (2003); Choi, *et al*. *Science* **324**, 63 (2009).

[2] A. V. Kimel *et al*., *Nature* **435**, 655 (2005); J. A. de Jong, *et al*. *Phys. Rev. B* **84**, 104421 (2011); J. Jiang, *et al*. *Appl. Phys. Lett*., **103**, 062403 (2013).

The following people are acknowledged for various contributions at different stages:
Dehui Sun, V. Ovidiu Garlea, Barry Winn, James Hester, Guochu Den, Shixun Cao, Yun Liu, Garry Mcintyre, Mark Hagen and Robert Robinson.

W-1-4 Controlling Skyrmions in Cu_2OSeO_3 through Doping; an insight to the relationship between crystal structure and magnetic ordering

M. Vás[a,b], J. Vella[a,b], A. Ferguson[a,b], C. Ulrich[c], S. Yick[a,b] and T. Söhnel[a,b]

[a] *School of Chemical Sciences, University of Auckland, Auckland, New Zealand.*
[b] *MacDiarmid Institute for Advanced Materials and Nanotechnology, Wellington, New Zealand*
[c] *School of Physics, University of New South Wales, New South Wales, Australia.*

Magnetic Skyrmion lattices (SkL) are spin ordering which are topologically protected due to their quantised winding number. This, along with other helimagnetic orderings offer a plethora of fascinating phenomena for fundamental research and applications.[1] Cu_2OSeO_3 is an insulating multiferroic material that has shown to host SkL at specific conditions.[2] It possesses a magnetic structure with both ferromagnetic (FM) and antiferromagnetic (AFM) super exchange interactions being present and has a 3-up 1-down ferrimagnetic arrangement of Cu^{2+} ions.[3] The lack of inversion symmetry in the corner shared O-Cu_4 tetrahedra lattice results in an appreciable DMI between Cu^{2+} sites; this competes with FM/AFM interactions leading to spin canting formation of helical/conical spin textures at different fields and temperature conditions.[2] Due to the absence of a crystallographic transformation throughout the temperature range alongside the formation of the magnetic phases, it has been commonly assumed that the structure plays a passive role in magnetic ordering.[3] Yet, published studies have challenged this assumption. The work by Wu *et al.* shows that internal expansion leads to a decrease in T_c for the helical to paramagnetic transition.[4] Furthermore, observation by Nishibori *et al.* shows that by applying a pressure, T_c increases as the unit cell volume contracts.[5]

In this work, we incorporated both magnetic and non-magnetic ions into the Cu_2OSeO_3 host. The inclusion of Te into the Se-sites and Co into the Cu-sites changed the crystal and magnetic structure, respectively. The skyrmion dynamics and spin interactions within these materials were then studied using synchrotron X-ray powder diffraction, neutron powder diffraction, and magnetometry. Using X-ray powder diffraction at the Australian synchrotron, we identify a structural anomaly where the Cu network distorts around the paramagnetic-helical ordering temperature. This alludes to the possibility that structure is also a contributing factor to the magnetic ordering of the material despite the lack of structural phase transition. Through neutron diffraction, we found that the magnetic response of the spin ordering is highly susceptible to chemical doping. This implies that the rigidity of the spin coupling might be affected by the both magnetic and non-magnetic dopants. We also studied whether doping changed the universality class through magnetometry. These results give us insight as to the relationship between materials structure and magnetic ordering. This highlights the importance of the crystal structure and an avenue to design novel spintronic materials.

[1] S. Mühlbauer, *et al.*, *Science* **323**, 915 (2009).
[2] S. Seki, *et al.*, *Science* **336**, 198 (2012).
[3] J.-W. G. Bos, *et al.*, *Phys. Rev. B* **78** (9), 094416 (2008).
[4] H. C. Wu, *et al.*, *J. Phys. D: Appl. Phys.* **48**, 475001 (2015).
[5] E. Nishibori, *et al.*, *Phys. Rev. B* **102**, 201106 (2020).

W-1-5 A semiempirical Hartree-Fock approach to solid-state calculations for inelastic neutron scattering

A.P.J. Stampfl

Australian Nuclear Science and Technology Organisation, Lucas Heights, NSW, Australia.

The scattering function, S(Q,ω), representing the interaction between the incident neutron and the pseudopotential, representing an ensemble of atoms, may be determined in a variety of ways: Via classical force-field approaches, through electronic structure calculations, through analytical approaches and through a combination of one or both of the first two approaches and applying molecular dynamics to study systems under non-equilibrium conditions. Electronic structure calculations quickly become computationally intensive and opaque once more than several hundred atoms are involved in a cluster or unit cell that represents the system under investigation.

In the case of neutron spectroscopy many systems investigated are dominated by hydrogen vibrations as the total scattering coefficient, total~82 Barn is approximately an order of magnitude larger than most total scattering coefficients from other elements. Scatter from hydrogen is mainly incoherent and therefore may be considered localised allowing potentially simple molecular models to be employed in the study of hydrogenous materials. Here, a well known Hartree-Fock semi-empirical calculation scheme is presented that is lightning fast for small molecules and adequate for large molecules, clusters, and dynamical studies.

Force constants are obtained by diagonalisation of the mass-weighted Hessian matrix to obtain the vibrational frequency for each mode assuming that each atomic-pair vibrates in a simple-harmonic fashion. The scattering function, S(Q, ω), is then calculated firstly assuming a one-atom oscillator, then secondly more thoroughly for each atom-pair vibration within the molecule/cluster, and finally as a weighted phonon density of states. A number of benchmark molecules are reported on. Interestingly, these rapid calculations give a very good estimation of the scattering function that can be used for initial peak identification and further analysis of the detailed electronic and vibrational structure.

W-2-2 Antiferromagnetism-driven Two-Dimensional Topological Nodal-Point Superconductivity

M. Bazarnika[a,b], R. Lo Conte[a], E. Mascot[a,c], K. von Bergmann[a], D. K. Morr[d], R. Wiesendanger[a]

[a] *Department of Physics, University of Hamburg, D-20355, Hamburg, Germany*

[b] *Institute of Physics, Poznan University of Technology, Piotrowo 3, 60-965, Poznan, Poland*

[c] *School of Physics, University of Melbourne, Parkville, VIC, 3010, Australia*

[d] *Department of Physics, University of Illinois at Chicago, Chicago, IL, 60607, USA*

Magnet/superconductor hybrids (MSHs) hold the promise to host emergent topological superconducting phases. Both one-dimensional (1D) and two-dimensional (2D) magnetic systems in proximity to *s*-wave superconductors have shown evidence of gapped topological superconductivity with zero-energy end states and chiral edge modes. Recently, it was proposed that the bulk transition-metal dichalcogenide 4Hb-TaS_2 is a gapless topological nodal-point superconductor (TNPSC). However, there has been no experimental realization of a TNPSC in a MSH system yet. Here we present the discovery of TNPSC in antiferromagnetic (AFM) monolayers on top of an *s*-wave superconductor. Our calculations show that the topological phase is driven by the AFM order, resulting in the emergence of a gapless time-reversal invariant topological superconducting state. Using low-temperature scanning tunneling microscopy we observe a low-energy edge mode, which separates the topological phase from the trivial one, at the boundaries of antiferromagnetic islands. As predicted by the calculations, we find that the relative spectral weight of the edge mode depends on the edge's atomic configuration. Our results establish the combination of antiferromagnetism and superconductivity as a novel route to design 2D topological quantum phases.

W-2-3 Non-Onsager Quantum Magnetic Oscillations

Zeb E. Krix, Oleg P. Sushkov

School of Physics, University of New South Wales, Sydney 2000, Australia.

Oscillation effects in crystals have been studied since the 1930s, when it was observed that a metal's magnetisation and resistance are periodic in the inverse magnetic field. Typically, the oscillation frequency corresponds to the area of a closed cross-section of the Fermi surface, these are Onsager oscillations. This effect became a standard way to map the Fermi surface of a metal. In this work we describe two new “non-Onsager” oscillation effects, that cannot be related to closed sections of the Fermi surface. We show that oscillations arise, in equilibrium, which survive to high temperatures and have a frequency related to the area difference between two sections of the Fermi surface. This effect is due to Coulomb interactions between electrons. We also develop a theory of so-called "fractional frequencies", which we show are due to disorder. We use this theory to explain recent experiments on two-dimensional artificial crystals.

W-2-4 Weyl excitations via helicon-phonon mixing in conducting materials

Dmitry K. Efimkin[a] and Sergey Syzranov [b]

[a] *School of Physics and Astronomy and ARC Centre of Excellence in Future Low-Energy Electronics Technologies, Monash University, Victoria 3800, Australia*

[b] *Physics Department, University of California, Santa Cruz, California 95064, USA*

Quasiparticles with Weyl dispersion can display an abundance of novel topological, thermodynamic, and transport phenomena, which is why novel Weyl materials and platforms for Weyl physics are being intensively looked for in electronic, magnetic, photonic, and acoustic systems. We demonstrate that conducting materials in magnetic fields generically host Weyl excitations due to the hybridization of phonons with helicons, collective neutral modes of electrons interacting with electromagnetic waves propagating in the material. Such Weyl excitations are, in general, created by the interactions of helicons with longitudinal acoustic phonons. An additional type of Weyl excitation in polar crystals comes from the interaction between helicons and longitudinal optical phonons. Such excitations can be detected in X-ray and Raman scattering experiments. The existence of the Weyl excitations involving optical phonons in the bulk of the materials also leads to the formation of topologically protected surface arc states that can be detected via surface plasmon resonance.

[1] D.K. Efimkin and S. Syzranov – *Phys. Rev. B* **108**, L161411 (2023)

W-2-5 Flat band engineering in Bernal-stacked Bilayer Graphene using Patterned Periodic Potential and Vertical Electric Field

Feixiang Xiang[a,c], Mudassar Nauman[b,c], Daisy Q. Wang[a,c], Abhay Gupta[a,c], Zeb E. Krix[a,c], Kenji Watanabe[d], Takashi Taniguchi[d], Oleg P. Sushkov[a,c], Alex R. Hamilton[a,c], Oleh Klochan[b,c].

[a] *School of Physics, University of New South Wales, NSW 2056, Australia.*
[b] *School of Science, University of New South Wales, Canberra ACT 2612, Australia.*
[c] *Australian Research Council Centre of Excellence in Future Low-Energy Electronics Technologies, University of New South Wales, Sydney 2052, Australia.*
[d] *National Institute for Materials Science, Tsukuba, Ibaraki 305-0044, Japan.*

The realization of a flat electronic energy band in materials is essential for the exploration of strongly correlated states, including superconductivity, magnetism, and Mott insulators [1-3]. Utilizing e-beam lithography-patterned superlattices to introduce external spatially periodic potentials provides a viable strategy for reconstructing band structures, with the potential to flatten energy bands [4-6]. This method not only facilitates the electrostatic tuning of periodic potential strength but also allows for the customized design of superlattice symmetry. Recent investigations into monolayer graphene have illuminated the impact of external periodic potentials induced by patterned superlattices, resulting in a strongly anisotropic band structure with a significant reduction in group velocity in specific superlattice directions [7]. However, creating an isolated flat band in monolayer graphene is challenging, primarily due to the inherent difficulty of opening a band gap.

In contrast to monolayer graphene, Bernal-stacked bilayer graphene exhibits a tunable band gap under a vertical electric field [8]. Numerous theoretical works have investigated the possibility of creating isolated flat bands with a combination of an external periodic potential and a vertical electric field [9,10]. In this study we investigate a bilayer graphene device featuring a graphite gate with a patterned square superlattice. This device enables the independent modulation of superlattice potential strength, carrier density, and the vertical electric field applied to the sample. Our transport measurements reveal that an increased modulation of the superlattice potential leads to the emergence of multiple secondary Dirac points. Furthermore, with a further increase in the vertical electric field, we observe clear evidence of gap opening at secondary Dirac points, with the band width between neighbouring gaps tunable by the vertical electric field. Our work shows the potential of bilayer graphene with patterned gates as a highly tunable platform for engineering flat bands and strongly correlated states.

[1] Y. Cao et al., *Nature* **556**, 80 (2018)
[2] Y. Cao et al., *Nature* **556**, 43 (2018)
[3] M. Serlin et al., *Science* **367**, 900 (2020)
[4] C.-H. Park et al., *Nat. Phys.* **4**, 213 (2008)
[5] C.-H. Park et al., *Phys. Rev. Lett*. **101**, 126804 (2008)
[6] D. Q. Wang et al., *Nano Lett.* **23**, 1705 (2023)
[7] Y. Li et al., *Nat. Nanotech.* **16**, 525 (2021)
[8] F. X. Xiang et al., *Nano Lett.* **23**, 9683 (2023)
[9] S. A. A. Ghorashi et al., *Phys. Rev. Lett.* **130**, 196201 (2023)
[10] Z. E. Krix et al., *Phys. Rev. B* **107**, 165158 (2023)

W-3-2 Crystal Structures of the Tungsten Bronzes

Christopher J. Howard

School of Engineering, University of Newcastle, Callaghan, NSW 2308, Australia.

The hexagonal and tetragonal tungsten bronzes (HTB, TTB) comprise networks of WO_6 octahedra providing tunnels for larger cations such as Ca or K (Fig. 1).

There is an expectation that different structures (with different space groups symmetries) might be formed by various patterns of tilting of the WO_6 octahedra, as practically rigid units.

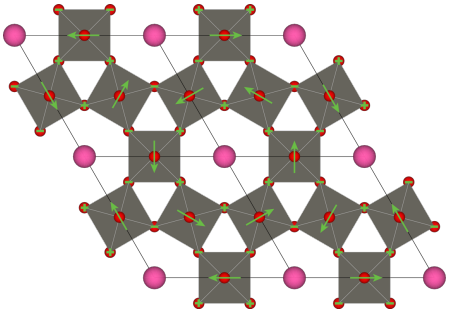

Fig. 1. Illustration of structure of idealised HTB, $M_{1/3}WO_6$.

Starting in late 2014, my colleagues and I tried to enumerate the different possibilities using a rather *ad hoc* approach [1], but our listing turned out to be incomplete. Subsequent attempts (unpublished) were not much more successful. Eventually, we developed a general method applicable to any configuration of linked rigid polyhedra [2,3]: we wrote equations for all the constraints that needed to be satisfied, linearized, and solved by the methods of linear algebra. Application of this method to the tungsten bronzes quickly led to a list of possible tilt systems [2,4], which was the solution to our original problem.

Due to linearization, results from the general method are guaranteed only for tilts of small magnitude. It proved possible to show [4] that at least one of the tilted tungsten bronze structures - and most likely more of them – could, by appropriate choice of lattice parameters and atomic coordinates, accommodate arbitrary angles of tilt. Work currently in progress (at Brigham Young University) is aimed at developing the general method to discover when larger tilt angles can be accommodated without polyhedral distortion. Evidently, the tungsten bronzes provide for critical testing of any procedure proposed.

[1] T.A.Whittle, S. Schmid and C.J. Howard, *Acta Cryst.* B**71**, 342-348 (2015).

[2] B.J. Campbell, C.J. Howard, T.B. Averett, T.A. Whittle, S. Schmid, S. Machlus, C.J. Yost and H.T. Stokes, *Acta Cryst.* A**74,** 408-424 (2018).

[3] B. J. Campbell, H. T. Stokes, T. B. Averett, S. Machlus, and C. J. Yost, *J. Appl. Cryst.* **54**, 1847-1856 (2021).

[4] T.A.Whittle, S. Schmid and C.J. Howard, *Acta Cryst.* B**74**, 742-744 (2018).

W-3-3 Mechanism for graphite formation: experiments, simulations and virtual reality

J.W. Martin, J. Fogg, G. Francas, K. Putman, C. Wood, E. Turner, I. Suarez-Martinez and N.A. Marks

Physics and Astronomy, Curtin University, WA 6102, Australia.

Graphite is one of the critical materials required to enable the energy transition. It is the anode material used in all lithium-ion battery chemistries and is where the lithium is safely stored when the battery is charged. However, graphite is highly energy intensive to produce due to the high temperatures required. Atomistic understandings are needed for determining the critical defects preventing graphite formation and how to remove them at lower temperatures and over shorter timespans. In this work, microscopy and computational approaches provide an atomistic mechanism for carbonised mesophase transforming into graphite [1,2]. High resolution transmission electron microscopy reveals the presence of screw dislocations in partially graphitising PVC. Molecular dynamics simulations provide insights into how an aligned mesophase gives rise to screws. The importance of alignment is explored for producing a graphite precursor instead of disordered carbon. The removal of screw dislocations are also explored and found to be due to edge dislocation gliding within a dislocation loop. The self-assembled simulations are explored using a new virtual reality game engine that allows for an atom's eye view of graphite forming. The visualiser runs within the Meta Quest virtual reality headsets and allows continuous exploration in a periodic simulation. These tools reveal further insights into edge reconstructions and defect geometries. While outstanding questions remain, the role of screw dislocations and their removal are critical for explaining graphite formation and provide new targets for producing graphite more cheaply. The virtual reality headset will be demonstrated after the presentation and during the break.

[1] Martin, Jacob W., et al. "Graphite rapidly forms via annihilation of screw dislocations." *Carbon* **215** 118386 (2023).
[2] Francas, Gabriel R., et al. "Topological defects and anisotropic development during pre-graphitization." *Carbon* **213** 118251 (2023).

W-3-4 Grains ain't misbehaving or going wild? The initiation of abnormal grain growth!

Klaus-Dieter Liss [a,*], Pingguang Xu [b], Ayumi Shiro [b,c], Shuoyuan Zhang [b,d], Eitaro Yukutake [e], Takahisa Shobu [b], Megumi Kawasaki [f], Koichi Akita [b,g]

[a] *School of Mechanical, Materials, Mechatronic and Biomedical Engineering, Northfields Avenue, University of Wollongong, NSW 2522, Australia;*
[b] *Materials Sciences Research Center, Japan Atomic Energy Agency, Tokai, Ibaraki 319-1195, Japan;*
[c] *Synchrotron Radiation Research Center, National Institutes for Quantum Science and Technology, Sayo, Hyogo 679-5148, Japan;*
[d] *Neutron Science and Technology Center, Comprehensive Research Organization for Science and Society, Tokai, Ibaraki, 319-1106, Japan;*
[e] *Industrial Technology Innovation Center of Ibaraki Prefecture, 3781-1 Nagaoka, Ibaraki-cho, Higashiibaraki-gun, Ibaraki 311-3195, Japan;*
[f] *School of Mechanical, Industrial and Manufacturing Engineering, Oregon State University, Corvallis, OR 97331, U.S.A.;*
[f] *Department of Mechanical Systems Engineering, Faculty of Science and Engineering, Tokyo City University, Tamazutsumi, Setagaya, Tokyo 158-8557, Japan;*

[*] *kdl@uow.edu.au*

Unconventional white-beam Laue synchrotron X-ray diffraction has been used on fine- and ultra-fine-grained, rolled magnesium alloys during in-situ heating experiments. At high temperatures, reflections of single grains are superimposed on the halo stemming from matrix grains. Some unique grain reflections spontaneously move, indicating grain rotations in response to torque expedited at grain boundaries. When a grain boundary spontaneously activates, the grain can begin to reorient, allowing diffusive mass transport and activating the boundaries of its other neighbors. Now the given grain can freely rotate towards coalescence; however, the multitude of grain boundaries compete in torque orientation and magnitude, resulting in zigzag rotations. After coalescence, the larger grain is still active and continues this scenario of growth, while the majority of the matrix grains remain inactive. The first-time experimental observation of such erratic grain behavior supplies the missing puzzle stone leading to abnormal grain growth, long postulated in literature. [1]

[1] Liss K-D, Xu P, Shiro A, Zhang S, Yukutake E, Shobu T, Akita K Abnormal Grain Growth: A Spontaneous Activation of Competing Grain Rotation. *Adv Eng Mater* n/a:2300470(1–9).https://doi.org/10.1002/adem.202300470

T-1-2 The role of atomic and structural disorder in the critical voltage scaling of Al/AlOx/Al Josephson junction arrays

Amanuel M. Berhane[a,b], Susan Coppersmith[b], Emma Mitchell[a], Tim Duty[b]

[a] *CSIRO Manufacturing, PO Box 218, Lindfield, 2070, NSW, Australia*.

[b] *School of Physics, University of New South Wales, 2052, NSW, Australia*.

A phenomenological study of atomic and nano-scale defects in Aluminium-Aluminium oxide-Aluminium (Al/AlOx/Al) Josephson junctions (JJs) will be presented. One-dimensional arrays of small capacitance JJs proved a valuable system for such a study, where the critical voltage (V_c) is a function of the junction parameters - the Josephson coupling energy (E_J) and the Cooper-pair charging energy (E_{CP}) [1, 2]. It will be shown that fabricating the junctions using the standard double-angle evaporation in the parallel direction (with respect to the chain) leads to larger V_c than junctions prepared using the perpendicular evaporation direction. The variability in the critical voltage is found to be due to nano-voids (gaps) introduced on each alternating junction along the series array when the second layer of Al film is deposited in the parallel evaporation direction. It was also observed that finishing the evaporation process with low-pressure oxygen termination before exposing the Al/AlOx/Al arrays to air reduces V_c, indicating a stoichiometric change in the glassy AlOx layer. While the variation in V_c is studied via low temperature (≈ 20 mK) DC measurements, the changes in the electrical properties of the arrays can be observed at room temperature (RT) via simple conductivity measurement. Scanning Electron Microscope (SEM) images are also used to correlate changes in film morphology and the presence of nano-scale defects at the junction to the observed variations in electrical properties. By studying material and process-related defects using nanostructured Al/AlOx/Al JJ arrays, this work proposes solutions to reduce sources of fluctuations in device parameters that limit the application of superconducting circuits for different applications, including quantum computing.

[1] D.B. Haviland, K. Andersson, P. Ågren, J. Johansson, V. Schöllmann, M. Watanabe, *Quantum phase transition in one-dimensional Josephson junction arrays*, *Physica C*: Superconductivity, **352** 55-60 (2001).

[2] K. Cedergren, R. Ackroyd, S. Kafanov, N. Vogt, A. Shnirman, T. Duty, *Insulating Josephson junction chains as pinned Luttinger liquids*, *Physical Review Letters*, **119** 167701 (2017).

T-1-3 The Unique Lattice Dynamics of Nanodiamond – a Molecular Dynamics and Inelastic Neutron Scattering Investigation

C. Stamper,[a] P. Galaviz,[b] K. Rule,[b] A. Bake,[a,c] K. Portwin,[a] S. Jin,[d] X. Fan,[e] M. Baggioli,[d] D. Yu[b*] and D. Cortie[a,b*]

[a]*Institute for Superconducting and Innovative Materials, University of Wollongong, Wollongong, Australia.*

[b]*Australian Nuclear Science and Technology Organisation, Lucas Heights, Australia.*

[c]*Institute for Glycomics, Griffith University, Brisbane, Australia.*

[d]*School of Physics and Astronomy, Shanghai Jiao Tong University, Shanghai 200240, China*

[e]*Shanghai National Center for Applied Mathematics, Shanghai Jiao Tong University, Shanghai 200240, China*

Nanoparticles exhibit remarkable properties owing to their size-dependent quantum effects and high surface-to-volume ratio. Among such particles, carbon-based nanoparticles stand out for their diverse and extreme properties. In particular, nanodiamond has gained a lot of attention due to its combination of extremely high surface-to-volume ratio (due to confinement in 3 dimensions), unique thermal, optical, and structural properties, and biocompatibility. Most recently, nitrogen-vacancy (NV) centres in nanodiamond have captivated the attention of researchers due to their potential use in quantum sensing, nanoscale imaging, thermometry, and more. Controlling and harnessing the intrinsic lattice vibrations (i.e., phonons) in nanodiamond, including their interaction with NV centres, is essential for advancing the capabilities of nanodiamond-based technologies.

To aid in the advancement of these technologies, we set out to provide a detailed description of the unique lattice dynamics of nanodiamonds through a synergistic approach involving inelastic neutron scattering (INS) and molecular dynamics (MD) simulations. This presentation highlights the observed distinctive vibrational modes available to nanodiamonds, compared with bulk diamond. Specifically, in our MD simulations, we observe the shifting and broadening of phonon modes in energy (acoustic and optical), excess vibrational modes at low energies leading to a deviation from a Debye relationship in the density of states, and excess vibrational modes at energies above the observed optical phonons. Many of these features are confirmed by INS measurements performed on Pelican. Our work underscores the significance of comprehending size-dependent lattice dynamics for harnessing the full potential of nanodiamonds in diverse technological applications.

T-1-4 Supported 2D-Coordinated Networks for CO_2 Reduction: Role and Influence of the Substrate

O.J. Conquest[a], Y. Jiang[b] and C. Stampfl[a]

[a] *School of Physics, The University of Sydney, NSW 2006, Australia.*

[b] *School of Engineering, Macquarie University, NSW 2109, Australia.*

The strong electron acceptor nature of certain metal coordinated molecules, together with their ability to form two-dimensional structures on supports, has recently been exploited for catalytic reactions [1,2]. In this work we study two-dimensional cobalt-coordinated Tetracyanoquinodimethane (Co-TCNQ) using density functional theory with GGA-PBE+D3 level of theory, the computational hydrogen electrode model, and a solvation entropy model [3,4]. Previous studies have shown that Co-TCNQ has a lower predicted overpotential for the CO_2 reduction reaction (CO_2RR) compared to other transition metal TCNQ coordination networks [5]. The CO_2RR performance is assessed by calculating the free energy reaction pathways, where we identify the role and influence of the substrate material. We consider copper, graphene, and pristine and defective diamond supports, and study their impact on the electronic properties of the cobalt active site of TCNQ which directly impacts the reaction performance. For the diamond substrate we consider a C vacancy, nitrogen vacancy (NV) and a boron substitutional (B_C) defect close to the surface. We find the NV defect for the neutral system and the B_C defect for the charged system have the largest impact on the predicted reaction performance. Further, we find that the application of strain and the varying charge state

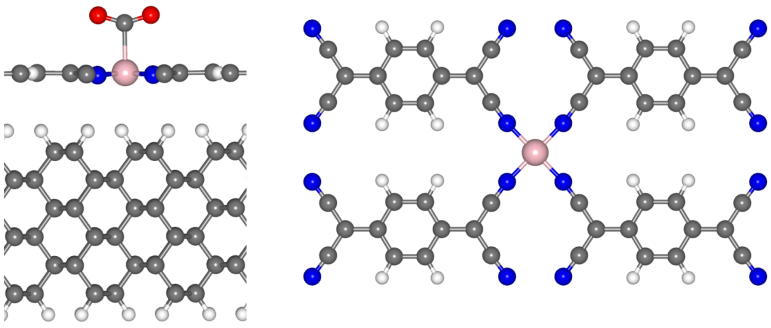

of the system can alter the potential determining step of the CO_2RR pathway, thereby suggesting approaches to improve the reaction performance.

Figure 1: Side view of adsorbed CO_2 on a charged (-1) Co-TCNQ coordinated network physisorbed on the diamond (110) substrate (left). Top view of the Co-TCNQ complex (right).

[1] X. Wang *et al., SmartMat*. **3**, 54-67 (2022)
[2] X. Yin *et al., Electrochimica Acta.* **443**, 141896 (2023)
[3] J. K. Norskov *et al.*, *J. Phys. Chem. B*, **108**, 46, 17886-17892 (2004)
[4] O. J. Conquest *et al.*, *J. Chem. Theory Comput.* **17**, 12, 7753-7771 (2021)
[5] E. Ganz *et al. J. Mater. Chem. A.* **7**, 3805 (2019)

T-1-5 Unravelling the local atomic order in the shear-bands of metallic glasses using scanning electron nano-diffraction

H. T. Pham[a], D. East[b], T.C. Petersen[c,a] and A.C.Y. Liu[a,c]

[a]School of Physics and Astronomy, Monash University, Clayton, Victoria 3800, Australia, [b]Advanced Manufacturing and Metals, CSIRO, Research Way, Clayton, Victoria, 3168, Australia, [c]Monash Centre for Electron Microscopy, Monash University, Clayton, Victoria, 3800, Australia.

Local atomic arrangements and local structural symmetry play a significant role in mechanical properties of globally disordered materials, such as metallic glasses [1]. However, the local atomic re-arrangements that govern deformation by shear banding remain unclear, even though this is an essential to understand brittleness and failure in metallic glasses. One promising approach for getting local structural information for glasses is to collect diffraction patterns from a small volume using full-field counting detectors and automated data acquisition. Recently, angular correlations in these small-beam diffraction patterns have been used to quantify different kinds of local structure in colloidal glasses prepared with different additives and after ageing and deformation [2,3,4].

Here, we investigate the local atomic structure of $Cu_{64}Zr_{36}$ metallic glasses before and after deformation using scanning electron nano-diffraction in a scanning/transmission electron microscope (S/TEM) (Figure 1). We spatially resolve the changes to the local structure from analysing the angular symmetries and distribution of intensity in the diffraction patterns to measure the local degree of centrosymmetry and the local structural anisotropy (strain). Furthermore, we also use monochromated electron energy-loss spectroscopy (EELS) to study vibrational modes in metallic glasses with high spatial resolution. Such atomic-level studies of structure and dynamics are necessary to understand the complex mechanisms of deformation in metallic glasses.

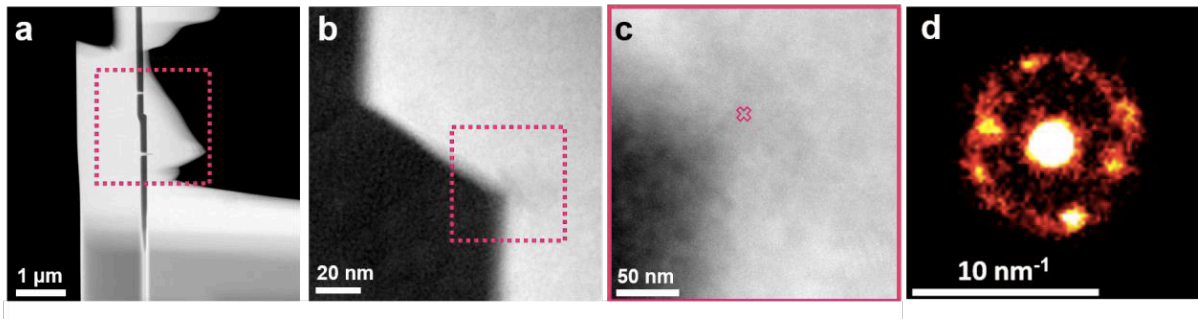

Figure 1. (a-c) STEM-HAADF images of shear-band area in $Cu_{64}Zr_{36}$. (d) nano-diffraction at area highlighted in a pink cross in panel c.

[1] E. D. Bøjesen, *et al.*, *J. Phys: Mater*. **3**, 044002 (2020).
[2] A. C. Y. Liu, *et al.*, *Proc. Natl. Acad. Sci*. **114**, 10344–9 (2017).
[3] A. C. Y. Liu, *et al.*, *Phys. Rev. Lett*. **116**, 205501 (2016).
[4] A. C. Y. Liu, *et al.*, *Sci. Adv*. **8**, eabn0681 (2022).

The authors acknowledge the use of the instruments at the Monash Centre for Electron Microscopy, a Node of Microscopy Australia. This research was supported by Australian Research Council (ARC) grants (LE0454166, FT180100594, LE200100132).

T-2-2 Universal van der Waals Electrodes Technology for Two-Dimensional monolayer Semiconductors

K. Xing[a,†], D. McEwen[a,b,†], M.S. Fuhrer[a,b]

[a] *School of Physics and Astronomy, Monash University, Clayton, Victoria 3800, Australia.*

[b] *Australian Research Council Centre of Excellence in Future Low-Energy Electronics Technologies (FLEET), Monash University, Clayton, Victoria 3800, Australia.*

Conventional electrode fabrication processes require high-energy metal atoms which induce significant defect states into the 2D semiconductors, resulting in the strong Fermi level pinning effect, low efficiency carrier injection, and large contact resistance. Transferring prepatterned metal contacts can resolve these issues but is limited only a few high-work function metals (Au, Pt, Pd). Most of the industry-preferred metals (such as Ti, Cr) show strong substrate adhesion and cannot be picked up easily with the standard dry transfer technologies. Here, we report a universal metal electrode pick-up technology to integrate van der Waals (vdW) contacts for monolayer semiconductors. Polished hydrogenated diamond substrates were utilized as reusable low-adhesion substrates for the fabrication of metal electrodes using standard lithography techniques (Fig.1). The metal electrodes are then transferred onto 2D semiconductors. The vdW interface between transferred electrodes and 2D semiconductors (WSe_2 and MoS_2) have been characterized using high-resolution transmission electron microscopy (HRTEM) to demonstrate the atomically clean interfaces. Eight candidates from low-work-function to high-work-function metals have been transferred with a high success rate. We investigate the device performance of monolayer TMDs with Pd, Bi, and Ti contacts to demonstrate our technique is suitable for high work function, semimetal, and low work function metal contacts. This technology has also been studied on the few layer TMDs with unsymmetric contacts to prove the minimal Fermi pinning effect. Our work not only realized vdW contacts for 2D monolayer semiconductors with a broad range of metals, but also paves the way for the wafer-scaled transferred electrodes compatible with commercial nanofabrication processes.

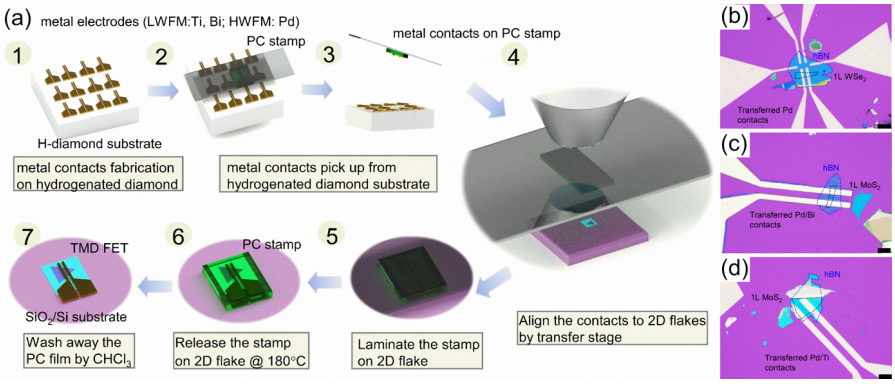

Fig. 1. (a) Schematic depicting the metal pick-up technique. 1. Metal contacts are deposited on H-diamond using standard photolithography techniques. A poly(bisphenol A carbonate) (PC) stamp is used to pick up the desired contact before transferring to the TMD FET. (b,c,d) Optical microscopy images of monolayer TMD FETs on hBN/SiO_2 with high work function Pd, semi-metallic Bi and low work function Ti transferred metal contacts.

T-2-3 Local tuning of Rydberg exciton energies in nanofabricated Cu_2O pillars

Anindya Sundar Paul[a,b,c], Sai Kiran Rajendran[b], David Ziemkiewicz[d], Hamid Ohadi[a], and Thomas Volz[c]

[a] *SUPA, School of Physics and Astronomy, University of St. Andrews, St. Andrews KY16 9SS, United Kingdom.*

[b] *Department of Physics and Astronomy, Macquarie University, Sydney, New South Wales, Australia.*

[c] *ARC Centre of Excellence for Engineered Quantum Systems, Macquarie University, Sydney, New South Wales, Australia*

[d] *Institute of Mathematics and Physics, Technical University of Bydgoszcz, and Al. Prof. S. Kaliskiego 7, 85-789 Bydgoszcz, Poland*

Rydberg excitons in Cuprous Oxide (Cu_2O) feature giant optical nonlinearities [1]. To exploit these nonlinearities for quantum applications, the confinement must match the Rydberg blockade size, which in Cu_2O could be as large as a few microns [2]. Here, in a top-down approach, we show how exciton confinement can be realised by focused-ion-beam etching of a polished bulk Cu_2O crystal without noticeable degradation of the excitonic properties. The etching of the crystal to micron sizes allows for tuning the energies of Rydberg excitons locally, and precisely, by optically induced temperature change. These results pave the way for exploiting the large nonlinearities of Rydberg excitons in micropillars for making non-classical light sources, while the precise tuning of their emission energy opens up a viable pathway for realizing a scalable photonic quantum simulation platform.

[1] Walther, Valentin, Robert Johne and Thomas Pohl. "Giant optical nonlinearities from Rydberg excitons in semiconductor microcavities." *Nature communications* **9.1** 1309 (2018).

[2] Kazimierczuk, T., Fröhlich, D., Scheel, S., Stolz, H. & Bayer, M. Giant Rydberg excitons in the copper oxide Cu_2O. *Nature* **514**, 343–347 (2014)

F-1-2 Realisation of epitaxial ultra-thin Kagome metal FeSn films

James Blyth[a], Mengting Zhao[a,b], Sadhana Sridhar[a], Grace Causer[a], Michael Fuhrer[a], Anton Tadich[b] and Mark Edmonds[a]*

[a]*School of Physics and Astronomy, Monash University, Clayton, VIC 3800 Australia*

[b] *Australian Synchrotron, Clayton, VIC 3168 Australia*

Kagome metals, a new class of metal, have recently attracted significant attention due to their rich topological, strong electron-correlated and magnetic properties [1]. These properties arise from the corner-sharing, triangular geometry that can facilitate both Dirac bands (massless electrons) and flat bands (massive electrons). The quantum anomalous hall effect (QAHE) and fractional-QAHE are believed to exist in 2D-isolated Kagome layers with spin-orbit coupling, leading to promising applications in ultra-low energy electronics [2-3] and quantum computing [4-5]. Though high-quality thin Kagome metal films have been realised, such as >20nm FeSn [6] and Mn_3Sn [7], large-area ultra-thin films have yet to be reported. Here, we report the successful growth of high-quality epitaxial ultra-thin FeSn films (<10nm) via molecular beam epitaxy. Structural characterisation reveals the Kagome lattice, with the expected lattice constant and correct 1:1 stoichiometry by X-ray photo-emission spectroscopy (XPS). Angular-resolved photo-emission spectroscopy (ARPES) measurements confirm the existence of Dirac bands at the K-points in the Brillouin Zone, where the extracted Fermi velocity of 1.3×10^5 ms^{-1} is consistent with bulk FeSn measurements [8]. The successful growth of ultra-thin Kagome metal films provides a pathway towards understanding the effect of quantum confinement on the electronic band structure, in particular, the opening of a bandgap in the Dirac bands and the realisation of novel quantum phenomena.

[1] Ye, L. et al. Massive Dirac fermions in a ferromagnetic kagome metal. *Nature* **555,** 638-642 (2018).
[2] Han, T.-H. et al. Fractionalized excitations in the spin-liquid state of a kagome-lattice antiferromagnet. *Nature* **492**, 406–410 (2012).
[3] Zhou, Y., Kanoda, K. & Ng, T.-K. Quantum spin liquid states. *Rev. Mod. Phys*. **89**, 025003 (2017).
[4] Jiang, Y.-X. et al. Unconventional chiral charge order in kagome superconductor KV_3Sb_5. *Nature Materials* **20**, 1353–1357 (2021).
[5] Shunli, N. et al. Anisotropic superconducting properties of kagome metal CsV_3Sb_5. *Chinese Physics Letters* **38**, 057403 (2021).
[6] Inoue, H., Han, M., Ye, L., Suzuki, T. & Checkelsky, J. G. Molecular beam epitaxy growth of antiferromagnetic kagome metal FeSn. *Applied Physics Letters* **115**, 072403 (2019).
[7] Higo, T. et al. Perpendicular full switching of chiral antiferromagnetic order by current. *Nature* **607**, 474–479 (2022). [8] Kang, M. et al. Dirac fermions and flat bands in the ideal kagome metal FeSn. *Nature Materials* **19**, 163–169 (2020).

F-1-3 Simulating angle-resolved photoemission intensity maps

T. Roman[a,b] and S.L. Harmer [a,b]
[a] *Flinders Microscopy and Microanalysis, Flinders University*
[b] *Institute for Nanoscale Science & Technology, College of Science and Engineering, Flinders University, Bedford Park, SA 5042, Australia*

Angle-resolved photoemission spectroscopy (ARPES) is a powerful technique that allows the direct observation of a solid crystal's electronic structure. ARPES intensity maps as a function of emitted photoelectron kinetic energy and wave vector k are often interpreted by overlaying calculated band structures on them, applying a slight energy offset to obtain a reasonable theory-experiment visual match. Nowadays, electronic band structures can be computed relatively quickly using Kohn-Sham density functional theory, an independent-electron method that returns allowed energy levels of an electron that moves in a periodic potential created by its interaction with atomic nuclei of the lattice and the surrounding sea of electrons.
But ARPES intensity maps provide even more information: fundamental many-body phenomena in an interacting Fermi-liquid system can be discovered through experimental signatures in the ARPES intensity. It is with the aim of a more accurate interpretation of photoemission data that several projects simulating ARPES intensity maps have been developed over the past decade [1–5]. In this talk we evaluate how well the tight-binding method is in reproducing photoemission maps for two 2D materials (graphene and MoS2) as well as for the fcc transition metals copper and gold.

[1] I. Gierz et al., *Physical Review B*, **83**, 121408 (2011).
[2] P. Puschnig, D. Lüftner, *Journal of Electron Spectroscopy and Related Phenomena*, **200**, 193–208 (2015).
[3] S. H. Park, S. Kwon, *Scientific Data*, **3**, 160031 (2016).
[4] R. P. Day et al., *npj Quantum Materials*, **4**, 1–10 (2019).
[5] M. Feidt et al., *Physical Review Materials*, **3**, 123801 (2019).

F-1-4 Protective ALD-Alumina Overlayer Prevents Agglomeration of Phosphine-Protected Au_9 Clusters on RF-TiO_2

M.Z. Asiri[a-d], H. Ebendorff-Heidepriem[a], G.F. Metha[b], G.G. Andersson[c]

[a]*Institute for Photonics and Advanced Sensing (IPAS) and the School of Physical Sciences, The University of Adelaide, Adelaide 5000, Australia.*

[b]*Department of Chemistry, University of Adelaide, Adelaide, South Australia 5005, Australia.*

[c]*Flinders Institute for Nanoscale Science and Technology and Flinders Microscopy and Microanalysis, College of Science and Engineering, Flinders University, Adelaide, South Australia 5042, Australia.*

[d]*Physics Department, Prince Sattam Bin Abdulaziz University, Al-Kharj 16278, Saudi Arabia.*

The research of gold metal clusters has recently been of great interest due to their potential in catalytic and photocatalytic applications including hydrogen production via water splitting. A noteworthy challenge is maintaining the cluster's size post-deposition, as they tend to agglomerate which results in the loss of their unique, size-dependent properties. Coating gold clusters with a metal oxide layer could be a suitable strategy to stabilise the clusters and prevent agglomeration. In the present work, phosphine protected Au_9 clusters deposited onto titania films were alternately exposed to H_2O and trimethylaluminum (TMA) by atomic layer deposition (ALD) to produce an ultrathin Al_2O_3 controlled overlayer. ALD layers were grown at 25° C, 120° C, 150° C and 180° C to determine the most suitable temperature for deposition to prevent agglomeration of the deposited Au_9 clusters. A range of techniques have been employed to characterize the deposited system of $Al_2O_3/Au_9/TiO_2$, including synchrotron x-ray photoelectron spectroscopy, x-ray photoelectron spectroscopy, angle resolved x-ray photoelectron spectroscopy, and neutral impact collision ion scattering spectroscopy.

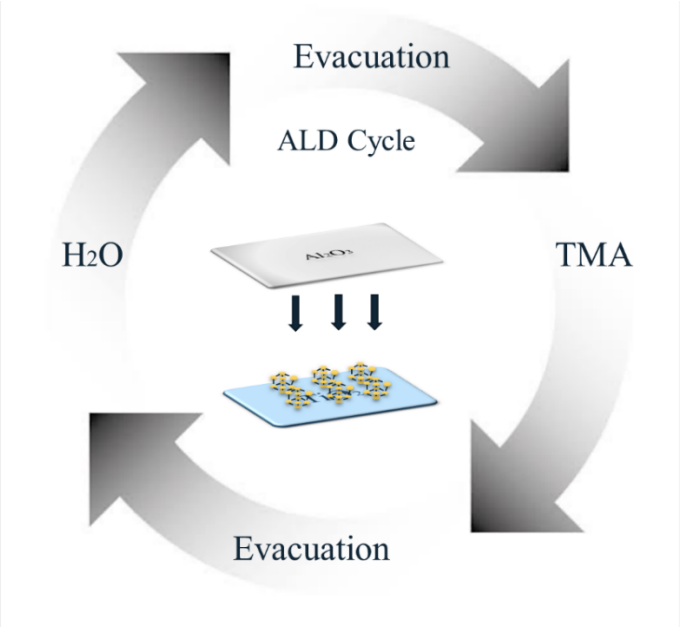

F-1-5 The phonon bandgap in thermoelectric SnSe: The role of dispersion interactions

Kyle A. Portwin [a], Caleb Stamper [a], Pablo Galaviz [b], Ramzi Kutteh [b], Dehong Yu [b], Kirrily C. Rule [a, b], Zhenxiang X. Cheng [a] and David Cortie [b]

[a] *Institute for Superconducting and Electronic Materials, University of Wollongong, Innovation Campus, Squires Way, North Wollongong, NSW 2500, Australia*

[b] *ANSTO, New Illawarra Rd, Lucas Heights NSW 2234, Australia*

In recent years, significant progress has been made in assessing the fundamental link between the phonon band structure and lattice thermal conductivity, illuminating a path towards materials with enhanced thermal properties. In this context, SnSe has emerged as an outstanding candidate for lead-free thermoelectric (TE) devices. Due to its ultra-low thermal conductivity, SnSe has demonstrated record-high TE performance, achieving a TE figure of merit, zT, of ~ 2.6 [1-3]. This performance is generally accredited to strong anisotropy, ultralow thermal conductivity, and large phonon anharmonicity. Several mechanisms have been proposed to explain the low thermal conductivity, including the unstable electronic structure or softening of low-energy optical phonon modes at the Brillouin zone centre [4-6]. However, these remain debated. To understand thermal conductivity, it is key to first characterize the underlying lattice dynamics, and the corresponding allowed phonon bands.

One of the distinctive features apparent in SnSe is the phonon band gap, i.e., a clear energy separation between the acoustic and optical bands. In other materials (e.g., boron arsenide [7]), a large phonon bandgap is crucial in suppressing phonon scattering. Nevertheless, the precise size and nature of the phonon bandgap in SnSe and the mechanistic understanding of these modes have yet to be established.

In this presentation, I will show results of inelastic neutron scattering and density functional theory experiments that clarify the size and origin of the phonon bandgap in SnSe and show that the size of this gap is sensitive to the type of dispersion force considered in the calculation.

F-2-2 Shape measurement by tracking topology in phase contrast and diffraction

T. C. Petersen[a], C. Zhao[a,b], E. D. Bøjesen[c], N. L. N. Broge[c], S. Hata[d], Y. Liu[e] and J. Etheridge[a,b]

[a] *Monash Centre for Electron Microscopy, Monash University, Victoria, Australia.*
[a] *School of Physics and Astronomy, Monash University, Victoria, Australia.*
[c] *Interdisciplinary Nanoscience Centre, Aarhus University, Midtjylland, Denmark.*
[d] *Department of Advanced Materials Science, Kyushu University, Fukuoka, Japan.*
[e] *Research School of Chemistry, The Australian National University, Canberra, Australia.*

Atomic resolution 3D imaging of biological specimens is now possible after decades of development for phase contrast electron microscopy, cryo-techniques (cryo-EM) and crucial electron detector advancements, since the first inception of electron tomography [1]. Comprising sensitive wave interference, phase contrast imaging of weakly interacting specimens is vital in this context for overcoming noise and mitigating irradiation damage. Coupled with sophisticated pre-processing, at the heart of such 3D reconstructions is the standard back-projection algorithm of computed tomography. Transmission electron microscopy is generally renowned for nanoscale 2D imaging afforded by strong electron-matter interactions. However, interpretation of specimen shape can be marred by overlapping detail in images, a problem which can be addressed with 3D reconstruction. Apart from cryo-EM, advanced incoherent electron imaging is often necessary to ensure accurate 3D back-projection reconstruction [2], subject to certain 'missing wedge' distortions from inaccessible specimen tilt orientations. Recent advances have enabled atomic resolution electron tomography of small nanocrystals [3]. For specimens for which only 3D *shape* is of interest, simpler 3D reconstruction methods are possible.

Here we describe a 3D imaging approach that can harness sensitive phase or diffraction contrast to measure 3D shape, and demonstrate this through electron microscope experiments across a variety of materials, including nanocrystals, alloys and cryo-EM specimens [4]. There exist a wide variety of specimens for which topological features of interest reside in phase contrast images, such as ridges, valleys, hills, saddles etc., and which are sparsely distributed. Our algorithm uses a differential geometry approach to stereoscopy, to track topological features within inline electron holograms, incoherent images, or diffraction patterns.

Fig. 1 shows two distinct examples: morphology of an isolated magnetite nanocrystal on a thick carbon support (a-c) and 3D diffraction from a complex perovskite $Pb(ScTa)_{0.5}O_3$. Both specimen reconstructions were measured from tilt series acquired on the FEI Titan 80-300 aberration corrected transmission electron microscope (at the Monash Centre for Electron Microscopy), operating at 300kV using plane wave illumination. The tilt series of specimen rotation angles spanned ±7.5º for the magnetite, sufficient to track the pertinent features, while the perovskite tilt angles spanned ±70º to minimise the missing wedge, which appears almost vertical in Fig. 1d and Fig. 1e. The continuum of diffracted intensities in Fig. 1d was reconstructed by assuming a flat Ewald sphere using bilinear interpolation, where the Bragg

peaks dominate the contrast. As shown by the 3D points in Fig. 1e, subtle diffuse streaks conveying correlated disorder were revealed by tracking topological features using our algorithm.

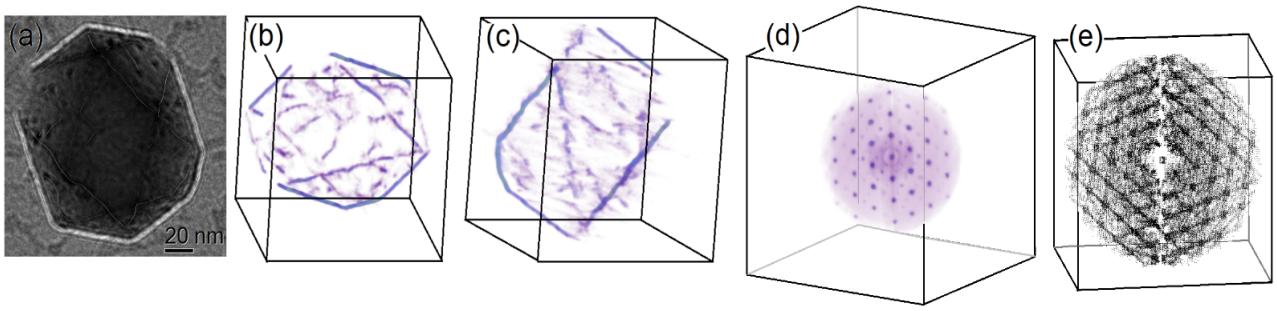

Figure 1. (a) magnetite nanoparticle in-line hologram with detected ridges and valleys overlayed in inverted contrast, with corresponding 3D reconstruction merging both ridges and valleys shown (b) & (c). $Pb(ScTa)_{0.5}O_3$ 3D diffraction of Bragg intensities is rendered in (d), with the 3D tracking-based reconstruction of topological ridges projected in (e).

[1] D. J. De Rosier and A. Klug, *Nature* **217**, 130 (1968)
[2] M. Weyland, P. A. Midgley and J. M. Thomas, *J. Phys. Chem. B* **105**, 7882 (2001).
[3] J. Miao, P. Ercius and S. J. L. Billinge, *Science* **353**, aaf2157 (2016).
[4] T. C Petersen, C. Zhao, E. D. Bøjesen, N. L. N. Broge, S. Hata, Y. Liu and J. Etheridge, *Ultramicroscopy* **236**, 113475 (2022).

This work was supported by the Australian Research Council (ARC) via grants LE0454166 and LE170100118, as well as the Japan Society for the Promotion of Science (JSPS)/Ministry of Education, Culture, Sports, Science and Technology (MEXT), Japan KAKENHI (JP18H05479, JP20H02426); Japan Science and Technology Agency (JST) CREST (\#JPMJCR18J4). Bo Brummerstedt Iversen of Aarhus University is thanked for support, along with that of the Villum Foundation. J. Etheridge acknowledges funding from ARC grant DP150104483. Matt Weyland and Laure Bourgeois are thanked for their assistance at the Monash Centre for Electron Microscopy.

F-2-3 Theoretical Modelling of 2D SQUID Arrays

O. A. Nieves[a], K.-H. Müller[a], M. A. Galí Labarias[b] and E. E. Mitchell[a]

[a] *CSIRO Manufacturing, Lindfield, New South Wales 2070, Australia*

[b] *AIST, Tsukuba Ibaraki 305-8568, Japan*

Superconducting quantum interference devices (SQUIDs) are used extensively in magnetic sensing applications due to their robustness and sensitivity [1]. Combining multiple SQUIDs into a grid-like structure, known as a SQUID or SQIF (superconducting quantum interference filter) array; has been shown to significantly improve the voltage-to-flux response of these devices [2], and theoretical models of these structures have also been developed for high-temperature superconductors [3]. Nevertheless, these models are based on the assumption that superconducting segments in the array are narrow compared to the hole sizes, hence neglecting flux focusing effects that arise in wider structures [4].

In this work, we model Yttrium-Barium Copper Oxide (YBCO) thin-film dc SQUID arrays at T=77 Kelvin and validate our results with experimental measurements. We demonstrate that the device's voltage response to externally applied magnetic fields cannot be accurately computed using traditional lumped element circuits when wide busbars are present in the array. This is because of flux focusing, which significantly modifies the effective area and mutual inductances between neighbouring loops. However, using Müller's stream function approach of solving London's equations along with the junction equations of motion [4]; we obtain accurate results for the voltage response which closely match experimental measurements.

[1] R. Kleiner, D. Koelle, F. Ludwig and J. Clarke, *Proceedings of the IEEE,* **92**, 10 (2004)
[2] J. Oppenländer, C. Häussler, T. Trauble, P. Caputo, J. Tomes, A. Friesch and N. Schopohl, *IEEE Trans. on Appl. Supercond.,* **13**, 2 (2003)
[3] M.A. Galí Labarias, K.-H. Müller and E.E. Mitchell, *Phys. Rev. Appl.,* **17**, 6 (2022)
[4] K.-H. Müller and E.E. Mitchell, *Phys. Rev. B*, **103**, 5 (2021)

F-2-4 Excitons in Atomically Thin TMD in Strong Magnetic Field

Jack Engdahl

School of Physics, UNSW Sydney

The large direct band gap and strong many body Coulomb interactions of atomically thin TMDs result in large exciton binding energies, making them ideal candidates for the study of exciton physics. However, in these types of systems there is discrepancy in the reported values of important system parameters such as reduced mass. In this work we derive an effective Hamiltonian to numerically solve for the excitonic energy and wavefunction of 2D excitons in a magnetic field, including spin-orbit interaction, and going beyond the simplified quadratic in magnetic field diamagnetic Hamiltonian often used for this purpose. We fit experimental data for a WSe_2 monolayer encased in hBN, extracting reduced mass $\mu = 0.165 \pm 0.005m_0$, dielectric constant $\varepsilon = 3.4 \pm 0.2\varepsilon_0$ and characteristic screening length $r_0 = 5.25 \pm 0.15$ nm/ε. Following the extraction of μ, ε and r_0, further theoretical investigation of exciton physics in WSe_2 may be performed.

POSTERS

Please display posters for the entire conference. Poster presenters should be available at their poster as follows:

Posters 1 to 9: Wednesday

Posters 10 to 17: Thursday

P1 Field-induced magnetic order of Sr_2RNbO_6 double perovskites, R = Ho, Er

Mustafa H. Ammar[a], Wayne Hutchison[a], Seán Cadogan[a] and James Hester[b]

[a] *School of Science, The University of New South Wales, Canberra, ACT 2600, Australia.*

[b] *Australian Centre for Neutron Scattering, ANSTO, Lucas Heights NSW 2234, Australia.*

At 'Wagga 2023' we reported on the crystal structure and magnetic properties of the 'double perovskite' series Sr_2RNbO_6 (R = Gd, Tb, Dy, Ho, Er and Tm). The samples were prepared via ceramic solid-state reaction with their crystal structures confirmed by X-ray powder diffraction and Rietveld refinement (using Fullprof [1]). In all cases these perovskites were found to be essentially single phase with the monoclinic $P2_1/n$ space group (#14_2) [2]. DC magnetisation as a function of temperature and magnetic field was measured using a Physical Property Measurement System (PPMS). Of particular note in the DC magnetisation was the observation of field-induced magnetic order, with a dip in the differential of the DC magnetisation data that was seen to shift to higher temperature with increasing magnetic field (in the range 0.2 to 5 T). In this paper we extend this study to neutron powder diffraction (NPD) on samples with R = Ho and Er using the *Echidna* HRPD at OPAL [3] to verify field-induced magnetic order at 1.7 K. The magnetic structures were determined via refinement of the NPD patterns using Fullprof to be canted ferromagnetic ("herringbone") arrangements. The NPD magnetic contributions are well fitted with a **k** = [000] propagation vector and magnetic order only at the R site. In the Ho case, the symmetry-allowed magnetic order is [FM, AF, FM], corresponding to the $P2_1'/n'$ (#14.79) magnetic space group, whereas the Er order is [AF, FM, AF], corresponding to the $P2_1/n$ (#14.75) magnetic space group. The different magnetic ordering modes correlate with the opposite signs of the respective crystal-field parameters of the R^{3+} ions. The "herringbone" order correlates with the tilting arrangement of the oxygen octahedra around the R sites and the concomitant crystal-field at the R^{3+} ions. In both cases, the magnitude of the R magnetic moments at 1.7 K and 5 T derived from NPD agree well with those observed from DC magnetisation.

[1] J. Rodriguez-Carvajal, *Physica B Condens. Matter* **192** 55-69 (1993).

[2] C. J. Howard, P. W. Barnes, B. J. Kennedy, P. M. Woodward, *Acta Cryst.* B**61**, 258-262 (2005).

[3] M. Avdeev and J.R. Hester, *J. Appl. Cryst*. **51**(6), 1597-1604 (2018).

P2 Valence states, magnetic and transport anisotropy in a new room-temperature 2D vdW Ferromagnet: Fe_3GaTe_2

Mengyun You[a,e], Yong Fang[b], James Hester[c], Weiyao Zhao[d,e], Abduhakim Bake[a,e], Kirrily C Rule[c,e] and Xiaolin Wang[a,e]

[a] *Institute for Superconducting and Electronic Materials (ISEM), University of Wollongong, Wollongong, NSW 2522, Australia.*

[b] *Jiangsu Laboratory of Advanced Functional Materials, Department of Physics, Changshu Institute of Technology, Changshu 215500, People's Republic of China.*

[c] *The Australian Nuclear Science and Technology Organisation (ANSTO), Lucas Heights, NSW 2234, Australia.*

[d] *Department of Materials Science & Engineering, Monash University, Clayton, VIC 3800 Australia.*

[e] *The Australian Research Council Centre for Excellence in Future Low Energy Electronics Technologies, Wollongong, Sydney, Melbourne, Australia.*

2D vdW ferromagnets are of interest as building blocks for heterostructures designed for use in spin-based information technologies because spin-orbit coupling within heterostructures generally yields interesting spin structures and magnetoelectric transport. For practical applications of 2D vdW ferromagnets in the next-generation spintronic devices, it is crucial for 2D materials to have magnetic states that are stable at room temperature [1]. No intrinsic 2D vdW ferromagnetic crystals with a room-temperature Curie temperature (*Tc*) were found until 2022 when 2D vdW ferromagnetic crystal Fe_3GaTe_2 was reported, showing *Tc* up to a record-high ~380K for known intrinsic vdW ferromagnets. These crystals were observed to have high M_{sat} 40.11 emu/g, large perpendicular magnetic anisotropy (PMA) energy density ~4.79×10^5 J/m^3, and a large anomalous Hall angle of 3% at room temperature. The PMA energy density of 2D Fe_3GaTe_2 nanosheet is ~ 3.88×10^5 J/m^3, which is better than some widely-used conventional ferromagnetic films such as CoFeB and Co_2FeAl, and one order of magnitude larger than other 2D vdW ferromagnets. The study also reported that room-temperature thickness and angle-dependent anomalous Hall devices based on Fe_3GaTe_2 nanosheet have been realized, which provides an avenue for next-generation magnetoelectronics and spintronics based on 2D vdW ferromagnetic crystals and various vdW heterostructures [2].

In this poster, we will give the first results of valence states of elements and magnetisation measurement of single crystal Fe_3GaTe_2. X-ray photoelectron spectroscopy (XPS) provides details on the chemical state, stoichiometry and Fermi level position by analysing XPS spectra with Avantage software. Magnetization measurement shows ferromagnetic properties with above-room-temperature *Tc* (~332-355K) under out-of-plane measurement.

P3 Does Iron have a Role in the Formation of Lightning Ridge Opals?

J D Cashion[a], B L Dickson[b], L P Aldridge[c], A Smallwood[d]

[a] *School of Physics and Astronomy. Monash University, Melbourne, Vic. 3800.*
[b] *47 Amiens St., Gladesville, NSW 2111.*
[c] *IFM, Burwood Campus, Deakin University, Vic 3125.*
[d] *International Opal Academy, P.O. Box 692, Sutherland, NSW 1499.*

The mechanism of the formation of opal is still a topic of some scientific conjecture. For example, it has been suggested[1] that the colour of Australian black opal is due to the incorporation of iron sulphides and carbon. To cast light on the first suggestion and to study the bonding of iron in opal, we have taken ^{57}Fe Mössbauer spectra of three opals. The optimum mass was chosen assuming that the sample was silica. The iron concentration was similar to that in the Be detector window and a spectrum of the window was used to correct each spectrum using a point by point addition. All spectra were counted for several weeks to >60 Mcounts/channel.

The first opal sample was a honey potch, which gave a spectrum with 0.1% dip and was fitted to three quadrupole split doublets. The largest (71%) is ferric in tetrahedral coordination[2], another ferric doublet (27%) is in the isomer shift gap between tetrahedral and octahedral and could be 5-fold coordination, while the third (14%) was ferrous with octahedral coordination. With a strong silica component in opal, tetrahedral coordination would have been expected.

The sample was then heated in air for 2 h at 700 ^{o}C to try to oxidize the ferrous component. Surprisingly, the two ferric components reduced in intensity, the dominant one from 71% to 50% and the other from 13% to 9%, while the original ferrous component disappeared to be replaced by two new components. One was ferrous and octahedrally coordinated with 25% of the area, while the other, with 16% could be ferric or valency 2.5, as in magnetite.

A black potch sample, with nominally the same iron concentration as the previous samples, gave a spectrum with a much larger maximum absorption of 0.3%, enabling better statistics. The principal doublet (55%) is probably ferric with uncertain coordination, the second is tetrahedral ferric (27%) and the remaining intensity is attributed to one, or possibly two, ferrous doublets. The increase in the size of the dip indicates stronger bonding. These samples show no evidence for iron sulfides in Lightning Ridge black opal but suggest the opal formed in a slightly reducing environment. Further spectra on other samples are in progress.

[1] Leechman, F, The Opal Book, (Ure Smith) 1969.

[2] Burns, R G and Solberg, T C, in Spectroscopic Characterization of Minerals and their Surfaces, Coyne et al., ACS Symposium Series, 1990, Chapt. 14.

P4 Enhanced magnetocaloric effect accompanying successive magnetic transitions in $TbMn_2Si_{2-x}Ge_x$ compounds

H.Y. Hao[a], W.Q. Wang[a], W.D. Hutchison[b], J.Y. Li[a], C.W. Wang[c], Q.F. Gu[d], S.J. Campbell[b], Z.X. Cheng[e] and J.L. Wang[a,b,e]

[a] *College of Physics, Jilin University, Changchun 130012, China*
[b] *School of Science, The University of New South Wales, Canberra, ACT 2600, Australia.*
[c] *National Synchrotron Radiation Research Centre, Hsinchu 30076, Taiwan*
[d] *Australian Synchrotron ANSTO, 800 Blackburn Rd, Clayton, Vic 3168, Australia*
[e] *Institute for Superconductivity and Electronic Materials, University of Wollongong, Wollongong, NSW 2522, Australia*

Magnetic refrigeration (MR) materials with a high magnetocaloric effect (MCE) [1] and large relative cooling power (RCP) in the temperature range required for hydrogen liquefaction (20 K to 77 K) is a gap in capability [2, 3]. The present investigation of $TbMn_2Si_{2-x}Ge_x$ compounds (x = 0.1, 0.2) by variable temperature neutron and synchrotron X-ray diffraction, magnetisation and heat capacity measurements, establish that substitution of Si with Ge in $TbMn_2Si_2Ge$ leads to a significant enlargement of the unit cell and modification of the magnetic properties. Two consecutive ferromagnetic first-order transitions occur below 77 K with a third transition from paramagnetism to a collinear antiferromagnetic state around 500 K. The resultant plateau-like MCE with large RCP below 77 K in these designed compounds offers scope for application for hydrogen liquefaction.

A detailed neutron investigation confirms that four magnetic states exist within the temperature range 5 K to 500 K, with two successive first-order magnetic transitions below 77 K being responsible for the large MCE. Our specific heat studies provide evidence of strong contributions from the nuclear specific heat and the corresponding nuclear specific heat coefficients of A = 430 ± 50 mJ mol^{-1} K^{-1} and A = 418 ± 60 mJ mol^{-1} K^{-1} have been determined for $TbMn_2Si_{2-x}Ge_x$ with x = 0.1 and 0.2, respectively. The overlapping entropy curves near these successive transitions lead to a plateau-like magneto-thermal effect as well as a large reversible MCE for both samples (e.g. DS_{Mmax} = 14.0 J kg^{-1} K^{-1} and DT_{max} = 7.6 K; with a RCP = 379 J kg^{-1} for $TbMn_2Si_{1.9}Ge_{0.1}$ for an applied field of 5 T) indicating that the material can operate over a wide temperature range, suitable for hydrogen liquefaction. [4]

[1] X. Tang, H. Sepehri-Amin, N. Terada, A. Martin-Cid, I. Kurniawan, S. Kobayashi, Y. Kotani, H. Takeya, J. Lai, Y. Matsushita, T. Ohkubo, Y. Miura, T. Nakamura and K. Hono, *Nat. Commun.* **13,** 1817 (2022).
[2] H.u. Zhang, R. Gimaev, B. Kovalev, K. Kamilov, V. Zverev and A. Tishin, *Physica B Condensed Matter* **558,** 65 (2019).
[3] K. Kamiya, K. Matsumoto, T. Numazawa, S. Masuyama, H. Takeya, A.T. Saito, N. Kumazawa, K. Futatsuka, K. Matsunaga, T. Shirai, S. Takada and T. Iida, *Appl. Phys Express* **15**, 5 (2022).
[4] H.Y. Hao *et al.*, *Journal of Magnetism and Magnetic Materials* **590,** 171654 (2024).

P5 Designing Multiferroic Heterostructures: A Density Functional Theory Study

F. Fakhera[a], O.J. Conquest[a], C. Verdi[b] and C. Stampfl[a]

[a] *School of Physics, The University of Sydney, NSW 2006, Australia.*
[b] *School of Mathematics and Physics, The University of Queensland, QLD 4072, Australia.*

Recently, multiferroic materials have attracted much interest in various novel electronic devices due to the co-existence of multiple ferroic orders, such as ferromagnetism (FM), ferroelectricity (FE), and ferro elasticity (FA). There are a variety of fascinating phenomena that are caused by the mutual coupling of various ferroic orders, providing new ideas for electronic devices of the future. In this study we use first principles calculations based on density functional theory to investigate $FeCl_2$ [1] and GaSe monolayers [2] for their ferromagnetic and ferroelectric properties, respectively, and their van der Waals heterostructures as a potential multiferroic material. We start by calculating the structural, electrical, and magnetic properties of the $FeCl_2$ and GaSe monolayers. Then we create the $FeCl_2$-GaSe heterostructure, investigating the materials tendency for ferroelectric distortions, particularly in the GaSe layer and a resulting coupled magnetic switching in the $FeCl_2$ layer. Finally, the magnetoelectric effect is also calculated by the reversal of electric polarizations between in-plane type and out-of-plane type orientations.

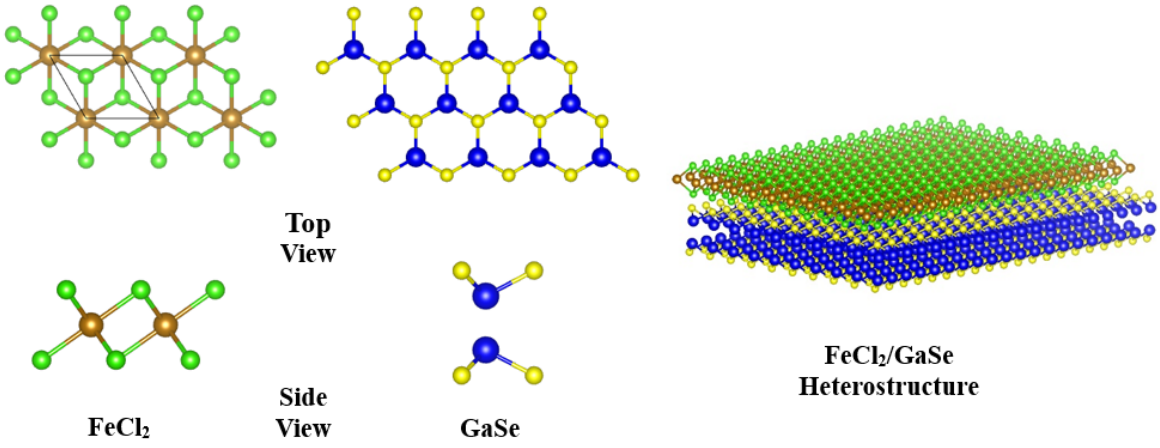

Figure: (a) Top and side views of the 2D $FeCl_2$ and GaSe monolayer, and (b) Crystal structure of 2D multiferroic $FeCl_2$/GaSe heterostructure. The green, brown, blue, and yellow represent Cl, Fe, Ga, and Se atoms, respectively.

[1] Zhou, Xuhan, *The Journal of Physical Chemistry C*. **124**, 9416-9423 (2020).

[2] Li, Wenhui, *Nature Communications* **14**, 2757 (2023).

P6 Neutron diffraction study on Co-based melilite compounds

M. Kawamata[a], M. Avdeev[b] and Y. Nambu[c, d, e]
[a] *Department of Physics, Tohoku University, Japan.*
[b] *Australian Nuclear Science and Technology Organisation, Australia.*
[c] *Institute for Materials Research, Tohoku University, Japan.*
[d] *FOREST, Japan Science and Technology Agency, Japan.*
[e] *Organization for Advanced Studies, Tohoku University, Japan.*

Layered transition metal oxides have attracted much attention owing to their interesting electronic and magnetic properties. The melilite structure $A_2XB_2O_7$ (A = alkali metals and lanthanides, X = transition metals, B = Si, Ge) generally has a tetragonal structure and XO_4 tetrahedra form two-dimensional network on the ab plane with B atoms between layers. They have a wide variety of magnetic structures, ranging from long-ranged commensurate magnetic orders to incommensurate magnetic orders [1]. Furthermore, these compounds are known to exhibit multiferroic properties with magnetic origins due to tilted antiferromagnetism and spiral magnetic structures induced by Dzyaloshinskii-Moriya interaction (DMI) associated with inversion symmetry broken structure.

$Sr_2CoSi_2O_7$ and $Sr_2CoGe_2O_7$ have the C-type antiferromagnetic magnetic structures with magnetic moments pointing to the ab-plane [2,3]. Recent neutron diffraction experiments on single crystalline samples of $Sr_2CoSi_2O_7$ [3] and isostructural $Ba_2CoGe_2O_7$ [4] have revealed the tilted antiferromagnetic structures, but the R factors for two magnetic space groups Cm′m2′ and P212′12′ are quite comparable and thus the magnetic structure has not yet been refined. Electric polarization measurements would be required to determine the intrinsic magnetic space group in these materials.

In this study, we performed neutron powder diffraction to refine magnetic structures of $Sr_2CoB_2O_7$ (B = Si, Ge), which is expected to have a magnetic structure canted by DMI due to its non-centrosymmetric structure. Using the powder diffractometer ECHIDNA at ANSTO, magnetic reflections were observed at the base temperature, 3 K. All magnetic reflections can well be indexed by the magnetic wavevector $\boldsymbol{q}_m$ = (0,0,0) r.l.u., and the magnetic space group was used for the magnetic structure refinement. In this presentation, we will give an overview, our experimental findings of the neutron powder diffraction and magnetic structure analysis, and will discuss the refined magnetic structures and their relations to DMI.

[1] H. Murakawa et al., *Phys. Rev. B* **85**, 174106 (2012).
[2] T. Endo et al., *Inorg. Chem.* **51**, 3572 (2012).
[3] R. Dutta et al., *Phys. Rev. B* **107**, 014420 (2023).
[4] V. Hutanu et al., *Phys. Rev. B* **89**, 064403 (2014).

P7 Electronic structures and microstructures in $La_3Ni_2O_7$ superconductors

Kaiyu Ma[a], Abudulakim Bake[a], Joshua Maggiora[b], Rongkun Zheng[b], Zhi Li[c], Meng Wang[d], Weiyao Zhao[e] and Xiaolin Wang[a*]

[a] *ISEM, University of Wollongong, NSW 2522*

[b] *School of Materials Science and Engineering, Faculty of Science, University of New South Wales (UNSW) Sydney, NSW 2052 AUSTRALIA,*

[c] *School of Materials Science and Engineering (E10, room 240) Faculty of Science, UNSW Sydney, NSW 2052 AUSTRALIA*

[d] *Center for Neutron Science and Technology, Guangdong Provincial Key Laboratory of Magnetoelectric Physics and Devices, School of Physics, Sun Yat-Sen University, Guangzhou, China*

[e] *Department of Materials Science and Engineering, Monash University, Wellington Rd, Clayton VIC 3800*

[*] *Corresponding author: xiaolin@uow.edu.au*

Superconductivity in cuprates has been widely observed and studied before. As an element with a similar atomic structure to the Cu^{2+} cation, Ni^{+} is expected to perform similar behaviour, and people have made extensive efforts to search for superconducting nickel-oxide compounds. Recently, a group from China reported that superconductivity occurred in Ruddlesden–Popper double-layered perovskite nickelate $La_3Ni_2O_7$ near 80K, 18.5GPa.

In this study, more comprehensive calculations and analyses of a $La_3Ni_2O_7$ were conducted based on density functional theory (DFT). We considered the situation with different external pressure and spin states of the Ni atoms, employed first-principles calculations to stimulate its material structure as well as phase transition, and found its band structure, density of state, and energy. The results which highly fit the experimental behaviour given by the original paper reveal the structural change and band structure shift of the $La_3Ni_2O_7$ lattice under different pressure and provide theoretical guidance to understand the origin of superconductivity of Nickel based superconductor. We will also present some results on TEM studies of the parent compound.

[1] Li, D. et al. Superconductivity in an infinite-layer nickelate. *Nature* **572**, 624–627 (2019).
[2] Sun, H., Huo, M., Hu, X. et al. Signatures of superconductivity near 80 K in a nickelate under high pressure. *Nature* **621**, 493–498 (2023). https://doi.org/10.1038/s41586-023-06408-7

P8 Mössbauer Effect Examination of Fe in $RFe_2Sn_2Zn_{18}$ (R = Nd, Pr, La)

Wayne D. Hutchison[a], Glen A. Stewart[a], Seán Cadogan[a] and Katsuhiko Nishimura[b]

[a] *School of Science, The University of New South Wales, Canberra, ACT 2600, Australia.*
[b] *Graduate School of Science and Engineering, University of Toyama, 930-8555, Japan.*

Compounds of the form RT_2M_{20} (R = rare earth, T = transition metal such as Ti, V, Cr and M = Zn or Al), are often referred to as *caged cubic compounds* as each R^{3+} ion is surrounded by 16 M ions and the spacing between the R ions is such that the usual RKKY interactions are weak. This results in a regime in which other effects can dominate. There has been considerable interest in these compounds because the hybridisation of the 4f moments and conduction electrons in these cubic structures have yielded a range of interesting low temperature properties. For example, superconductivity, Kondo effect and quadrupolar order are observed for the Zn-based RX_2Zn_{20} and the aluminium based RX_2Al_{20} compounds [1-3].

The focus of this paper is the related series, $RT_2Sn_2Zn_{18}$. These compounds, first studied by Isikawa *et al.*, are analogous to the Zn_{20} materials with the Sn atoms incorporated via a mixed-metal flux growth method and perhaps occupying a single crystallographic site (16c) in the Fd $\bar{3}$m cubic structure [4]. Their comprehensive work included observation of anomalously large heat capacity at very low temperatures (< 1 K) especially in R = Pr, T = Fe compounds. The authors, suggest these large specific heats could be due in part to spin frustration of the Fe spins (Fe in the 16d, $\bar{3}$m positions, carry a moment in similar compounds [5]). A longer-term aim is the use ^{57}Fe Mossbauer spectroscopy at very low temperatures to examine this suggestion. However, an alternative approach on the anomalous specific heat behaviour may be to consider the 'rattling' of the R and other atoms e.g. Zn or Sn substitutional in the 16d sites [6]. It is important to establish firstly whether the site occupancy, especially of the Sn, is as suggested by [4]. Our preliminary ^{57}Fe Mossbauer measurements show a considerably larger electric quadrupole interaction in the case of the Sn containing compounds than might be expected for purely Zn_{20} cases.

[1] T. Onimaru *et al.*, *J. Phys. Soc. Jpn*. **79**, 033704 (2010).
[2] T. Onimaru *et al.*, *Phys. Rev. B* **86**, 184426 (2012).
[3] M. Tsujimoto *et al.*, *Physical Review Letters* **113**, 267001 (2014).
[4] Y. Isikawa *et al.*, *J. Phys. Soc. Jpn.* **84**, 074707 (2015).
[5] I. Tamura *et al.*, *J. Phys. Soc. Jpn.* **82**, 114703 (2013).
[6] R. White *et al.*, *J. Alloys & Compounds*, **845** 156184 (2020).

P9 Small-beam diffraction measurements for understanding local structure and local dynamics in glasses

A.C.Y. Liu[a,b], E. Bøjesen[c,b], S.T. Mudie[d], R.F. Tabor[e], A. Zaccone[f], P. Harrowell[g] and T.P. Petersen[b,a]

[a] *School of Physics and Astronomy, Monash University, Victoria 3800, Australia.*
[b] *Monash Centre for Electron Microscopy, Monash University, Victoria, 3800, Australia.*
[c] *Interdisciplinary Nanoscience Centre and Centre for Integrated Materials Research, Aarhus University, Aarhus C 8000, Denmark.*
[d] *Australian Synchrotron, ANSTO, Clayton, Victoria 3168, Australia.*
[e] *School of Chemistry, Monash University, Victoria 3800, Australia,*
[f] *Department of Physics, University of Milan, Milan, Italy.*
[g] *School of Chemistry, University of Sydney, Sydney, N.S.W. 2006, Australia.*

In centrosymmetric crystals, each atom is at a centre of symmetry and thus at mechanical equilibrium, with the forces balanced by all its neighbours. Under an applied force, the particles undergo affine displacements that are proportional to this force until the elastic limit is reached, and topological defects are created. In dense glasses with isotropic interparticle interactions (e.g. metallic and colloidal glasses) the local environment around any given particle is generally not a symmetric polyhedron and the imbalance of forces results in irreversible, non-affine displacements [1]. The nature of the local structures that undergo these displacements under mechanical loading, or "flow defects", in glasses is not known.

In this study, we make a direct link between local stability and local structure in a glass using scanning microbeam small-angle x-ray scattering [2]. We employ micro-x-ray cross-correlation measurements [3] to resolve spatial variations in local structural dynamics. We analyze the angular symmetries and distribution of intensity in the speckle diffraction patterns to measure the local degree of centrosymmetry and the local structural anisotropy or strain [2]. Our measured maps of stability and structure demonstrate that even though local stability and local centrosymmetry fluctuate at the length scale of a single polyhedron, the structural centrosymmetry is still a strong predictor for mechanical stability in glasses. We examine local stability and structure during glass aging and deformation and find that coordinated local structural transformations to lower symmetry structures are central to these phenomena [2]. This provides new particle-level insight into these unique glass behaviours. Analogous scanning electron nanodiffraction measurements may give new insight into atomic glasses.

[1] Schlegel, M., Brujic, J., Terentjev, E. M., Zaccone, A., *Sci. Rep*. **6**, 18724 (2016).
[2] Liu, A. C. Y., Bøjesen, E.D., Tabor, R.F., Mudie, S. T., Zaccone, A., Harrowell P. and Petersen, T. C., *Sci. Adv.,* **8**, eabn0681 (2022).
[3] Hurley, M. M. and Harrowell, P., *J. Chem. Phys.* **107**, 8586–8593 (1997).

This research was undertaken on the SAXS/WAXS beamline at the Australian Synchrotron, Victoria, Australia. We thank J. Etheridge, L. Bourgeois, D. Paganin, T. Davis and A. Martin for discussions. A.C.Y.L. acknowledges support from the Monash Centre for Electron Microscopy and the Australian Research Council (FT180100594). E.D.B. acknowledges financial support from the Villum Foundation (VKR023371) and the Australian Research Council (DP150104483).

P10 PELICAN –a Time of Flight Cold Neutron Spectrometer – Recent Scientific Outcomes and New Capabilities

Dehong Yu and Richard Mole

Australian Centre for Neutron Scattering, Australian Nuclear Science and Technology Organisation, New Illawarra Road, Lucas Heights, 2234, Australia

The time-of-flight direct-geometry neutron spectrometer, Pelican, has been in user program since 2014 at the OPAL research reactor, at the Australian Nuclear Science and Technology Organisation (ANSTO) [1]. The Pelican instrument was designed to meet the diverse requirements of the Australian scientific community from physics, chemistry, material science, to biology. A wide range of research fields is covered. These include crystal-field excitations, phonon densities of states, magnetic excitations for various multifunctional materials including high Tc superconductors, novel magnetic, thermoelectric, ferroelectric and piezoelectric materials; molecular dynamics in hydrogen-bonded and storage materials, catalytic materials, cements, soils and rocks; and water dynamics in proteins and ion diffusion in membranes. Polarized neutrons and polarisation analysis option makes the full use of the neutron spin to study magnetism and to separate the coherent and incoherent scatterings.

In this presentation, the recent scientific outcomes and recent developments of new capabilities of the instrument will be demonstrated with several systems studied using quasi-elastic and inelastic neutron scatterings. These include water dynamics around amino acids, crystal field excitations in magnetic molecular crystals, low energy magnetic excitations in spin frustrated magnet, oxygen diffusion in solid oxide conductors and phonon density of states in energy materials. To meet the demand of diverse user community, new sample environment equipment has been developed and commissioned including high pressure cell, in-situ light irradiation, fast dilution temperature cooling system and superconducting magnet. The upgrade of the instrument with focusing guides and further test of the polarisation system will be highlighted.

[1] D. Yu, R. Mole, T. Noakes, S. Kennedy and R. Robinson, *J. Phys. Soc. Jpn.,* **82**, SA027 (2013).

P11 Significant reduction of thermal conductivity of intermetallic Mg_2Si thermoelectric material from carbon fiber inclusion.

Md Rezoanur Rahman[a,b], Sheik Md Kazi Nazrul Islam[a,b], David Cortie[a,c], Caleb Stamper[a] , Al Momin Md Tanveer Karim[a] , Xiaolin Wang*[a]

[a] *Institute for Superconducting and Electronic Materials (ISEM), University of Wollongong, New south Wales, 2500, Australia.*

[b] *Commonwealth Scientific and Industrial Research Organization (CSIRO), Victoria, 3195, Australia.*

[c] *Australian Nuclear Science and Technology Organization (ANSTO), New south Wales, 2234, Australia.*

Thermoelectric power generation, which utilizes dispersed waste heat energy, has garnered interest as a durable and eco-friendly power source. Mg_2Si-based alloys show great potential as thermoelectric materials for converting energy in the intermediate to high temperature range. The thermoelectric performance of Mg_2Si has been improved using techniques such as impurity doping, nano-structuring, and alloying. Additionally, they have the potential to lead to a decrease in the weight of thermoelectric generators, which is a crucial characteristic for the automotive industry. To decrease the thermal conductivity of silicide-based materials, one can modify phonon scattering by introducing nanosized crystalline grains. This work investigates the impact of Carbon Fiber-doping and small quantities of the isoelectronic impurity carbon fiber (CF) on the thermal characteristics of magnesium silicide (Mg_2Si). The study focused on examining the impact of different levels of Carbon fiber doping on Mg_2Si (specifically, Mg_2Si:CF=1:x where x represents the doping amount of 0.0025, 0.005, 0.0075, 0.01, and 0.05 ratio).

This work produced compact polycrystalline samples of Mg_2Si by Spark Plasma Sintering techniques. The materials' shape, content, and structure were studied using SEM, EDS, and XRD investigations following each step of the process. This work presents an analysis of the thermal conductivity of the samples which analysis using Laser flash analysis techniques. However, CF did decrease the thermal conductivity significantly and we achieved lowest thermal conductivity till date for Mg_2Si. Approximately, 68.44% thermal conductivity reduced by doped Mg_2Si at room temperature compared to undoped Mg_2Si we produced in our laboratory as well as 53.61% reduction compared to reported Mg_2Si undoped samples[1]. Additionally, thermal conductivity of 5 wt.% CF Mg_2Si showed up to 30.67% reduction at room temperature and 56.92% reduction at 773 K compared to reported Sb and C co-doped Mg_2Si [2].

1. Li, J., et al., *Enhanced thermoelectric performance of high pressure synthesized Sb-doped Mg_2Si. Journal of Alloys and Compounds*, **741** 1148-1152 (2018).
2. Shiojiri, D., et al., *Enhancement of thermoelectric performance of Mg_2Si via co-doping Sb and C by simultaneous tuning of electronic and thermal transport properties. Journal of Alloys and Compounds*, **891** 161968 (2022).

P12 Recent neutron polarisation analysis experiments at ACNS

Kirrily Rule[a], Nicolas de Souza[a], David Cortie[a], Andrew Manning[a] and Shinichiro Yano[b]

[a] *Australian Centre for Neutron Scattering, ANSTO, NSW 2234, Australia.*

[b] *National Synchrotron Radiation Research Centre, Hsinchu, Taiwan.*

A number of recent neutron scattering experiments at ACNS have used polarisation analysis with ^{3}He spin filters in novel ways to achieve interesting experimental outcomes. An experiment was carried out on the cold triple-axis spectrometer Sika to complement a previous quasi-elastic neutron scattering study of a polyelectrolyte undertaken on the backscattering instrument Emu, but in this case the separation of coherent and incoherent scattering (the latter dominated by hydrogen dynamics) was achieved with polarisation analysis. Another experiment used a custom-designed magnetic insert to produce a 0.3 Tesla horizontal field for a terbium iron garnet sample to investigate the Spin Seebeck Effect on the thermal triple-axis spectrometer Taipan, while a further experiment on Taipan measured the anti-ferromagnetic structure of a PtMn crystal at high temperature using a vacuum furnace. Recent measurements undertaken on Platypus to test off-specular polarised neutron reflectivity capabilities, as well as some current work to upgrade various instrumentation, will also be described.

P13 Removing Defect States from a Visible Light Photocatalytic Semiconductor for Solar Hydrogen using Atomic Layer Deposition of an Al_2O_3 Passivating Overlayer.

M. Smith[a] and G. Andersson[a]

[a] *College of Science and Engineering, Flinders University, South Australia*

Nitride and sulfide-based perovskite semiconductors are promising candidates for photocatalytic semiconductor based solar hydrogen production; their low bandgap should theoretically allow the efficient use of an appreciable portion of the solar spectrum [1]

However, their practical limitations remain for these materials; prime amongst them the high level of defect states existing within both the materials bandgap as a result of chemical alteration during manufacture and disruption to their crystal lattice limits their actual efficiency under simulated solar and UV irradiance [2]

In other contexts Atomic Layer Deposition (ALD), a method of depositing a one atom thick overlayer onto a material has been used to passivate similarly defect prone surfaces successfully [3] We present, to the best of our knowledge, the first study investigating the possibility of applying this technique to remedy the defect states in narrow bandgap photocatalytic semiconductors.

6 samples of the semiconductor $BaTaO_2N$ were in nanoparticle form and drop cast to a SiO_2 surface taken. The samples were then subjected to Ultraviolet Photoelectron Spectroscopy (UPS) to approximate the density of state function associated with that material's bandgap energies (and thus how many defects exist on the surface) immediately after drop casting, after 1 layer of Al_2O_3 was applied and then again after 3 layers of Al_2O_3 was applied.

The UPS data was then evaluated qualitatively and quantitatively to determine the change in the density of states within the band gap of $BaTaO_2N$ upon deposition of the Al_2O_3 layers. It was found both qualitatively and statistically that the deposition of deposition of three Al_2O_3 layers decreases the number of measured defects.

These findings suggest that ALD can be used to passivate defects in some narrow bandgap semiconductors a finding which could help pave the way toward high-efficiency use of narrow bandgap semiconductors.

1. Shraddha, J., et al., *Efficient photocatalytic oxygen evolution using $BaTaO_2N$ obtained from nitridation of perovskite type oxide. Journal of Materials Chemistry A*, **38** 1127 (2020).
2. Yamakata, A., J. Vequizo, and M. Kawaguchi, *Behavior and Energy State of Photogenerated Charge Carriers in Single-Crystalline and Polycrystalline Powder $SrTiO_3$ Studied by Time-Resolved Absorption Spectroscopy in the Visible to Mid-Infrared Region. The Journal of Physical Chemistry*, **119** 1880 (2015).
3. Berghuis, W., et al., *Surface passivation of germanium by atomic layer deposited Al_2O_3 nanolayers. Journal of Materials Research* **366** 571 (2021).

P14 DFT WIEN2k Generated Scattering Factors for lattice contraction studies employing QCBED in light metals

Andrew E. Smith[a], Tianyu Liu[b] , Philip N.H. Nakashima[b], Laure Bourgeois[b] , Z. Zhang[c]

[a] *School of Physics and Astronomy, Monash University, Victoria 3170, Australia.*
[b] *Department of Materials Engineering, Monash University, Victoria 3170, Australia.*
[c] *EMAT , Univ. Antwerp, NANOlab, Univ. Antwerp, Groenenborgerlaan 171, 2020 Antwerp, Belgium: Dept. of Materials, Univ. Oxford, 16 Parks Road, Oxford OX1 3PH, UK.*

Quantitative Convergent Beam Election Diffraction (QCBED) is a well-established experimental method providing unique insights into electron bonding and material strength [1]. It relies on the input of electron scattering factors into the computational analysis of the electron scattering process, whether by Bloch wave or multi-slice formulation. Scattering factors from the superpositions within the canonical Doyle Turner (DT) tables initiate the Nakashima and Muddle QCBED algorithm [1]. The Bonding Density in Aluminum has been established through comparison of results from QCBED with the DFT WIEN2K [3] computer package [1,2]. DT scattering factors can be replaced by those from an Independent Atom Model (IAM) determined from WIEN2K, not on a finite crystalline lattice, but instead on a lattice, with atoms notionally infinitely distant from one another.

IAM scattering factor calculations are analogous to calculations used in WIEN2K for crystal binding energies [3]. Developments of the methods for large cells (especially cubic symmetry) cases have been aided by recent improvements in WIEN2K. Similarly, scattering factor calculations of slab geometries and supercells are analogous to calculations in WIEN2K that determine surface energies and displacements. This paper discusses recent results of WIEN2K calculations of aluminium lattice contraction factors as function of vacancy concentration.

[1] P.N.H. Nakashima, "*The Crystallography of Aluminum and Its Alloys*" in Encyclopedia of Aluminum and Its Alloys ed. George E. Totten, Murat Tiryakioğlu and Olaf Kessler (Boca Raton: CRC Press,16 Nov 2018), 488 – 586.
[2] P.N.H. Nakashima, A.E. Smith, J. Etheridge, B.C. Muddle, *Science* **331 (6024)**, 1583-1586 (2011).
[3] P. Blaha, K. Schwarz, G.K.H. Madsen, D. Kvasnicka, J. Luitz, R. Laskowski, F.Tran, L.D. Marks. *WIEN2k, An Augmented Plane Wave + Orbitals Program for Calculating Crystal Properties.* (Vienna: Karlheinz Schwarz, Techn. Universität Wien, 2022).

P15 Terahertz Spectroscopy for Polyethylene Terephthalate (PET) Recycling

T. J. Sanders[a,b], J. L. Allen[a], J. Horvat[a] and R. A. Lewis[a]

[a] *School of Physics, University of Wollongong, New South Wales 2522, Australia.*

[b] *Australian Synchrotron, Australian Nuclear Science and Technology Organisation, Clayton, Victoria 3168, Australia.*

Plastics present a major challenge of the 21st century as they are prolific but produced from a non-renewable source (crude oil) and can cause many environmental problems [1]. While reducing the global reliance on plastics is part of the solution, plastics are still necessary in some fields, for example in preserving sterile medical supplies. Thus, improving current recycling methods is still a valuable endeavour. Terahertz spectroscopy is a maturing technique for probing the vibrational modes of materials in a non-ionising, non-destructive manner that may be used to discern different plastic samples. Firstly, characteristic features need to be identified that can be used as markers to distinguish different plastics. This work focuses on identifying these characteristic features in polyethylene terephthalate (PET) by studying the terahertz spectrum.

Spectra have been collected on the terahertz beamline at the Australian Synchrotron. Fourteen samples of PET plastic from everyday household items have been studied, discerned by their plastics identification code, along with a commercially purchased biaxially orientated sample (BO-PET). The BO-PET sample is more crystalline than standard PET and acts as a reference point for the other samples studied. The samples have been investigated in a variety of ways to determine the suitability of terahertz spectroscopy in their spectroscopic identification. Firstly, the most intense terahertz source of radiation has been used. Next, low temperatures and polarisation dependence have been investigated for additional insight into the spectra. The results, summarised in Fig. 1, show that while there is much variety in commercial PET, there are common absorptions. These features can be used to identify PET amongst other plastics.

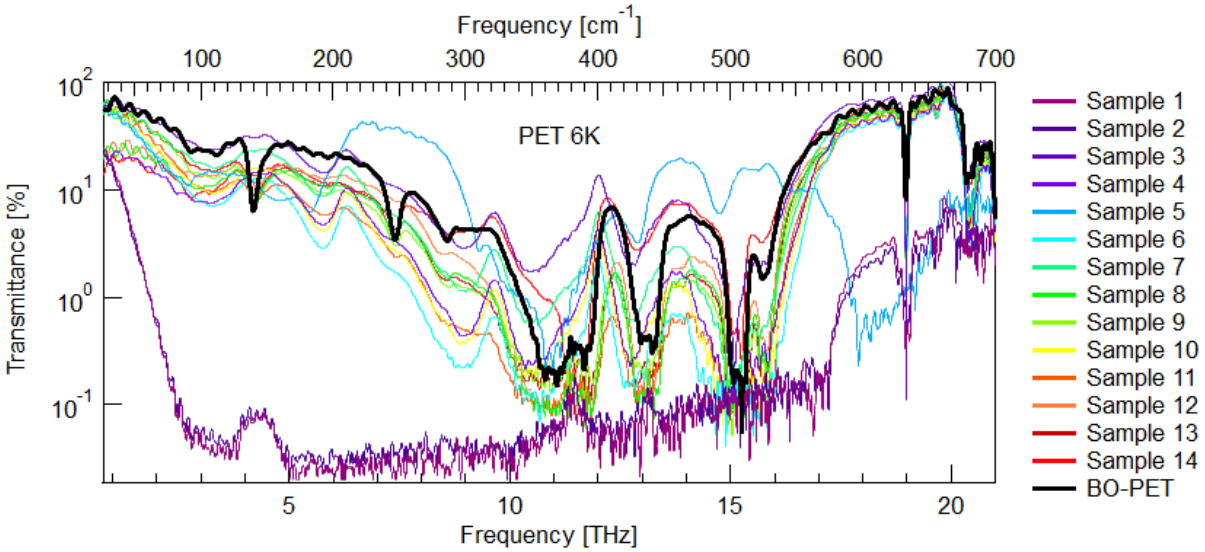

Figure 1: The terahertz spectrum of 12 commercially available samples of PET and the BO-PET sample, at 6K.

[1] J. Costa, P. Santos, A. Duarte and T. Santos, *Sci. Total Environ.* **566-567**, 15-26 (2016).

P16 Towards Observing Exciton-Polariton Rydberg Blockade in Cuprous Oxide

H. H. Vallabhapurapu[a], Anindya Sundar[b], Sai Kiran Rajendran[b], Hamid Ohadi[b], Thomas Volz[a]

[a] *School of Mathematics and Physical Sciences, Macquarie University, Sydney, Australia*
[b]*SUPA, School of Physics and Astronomy, University of St Andrews, St Andrews, UK*

Researchers in quantum optics are exploring ways to create strong interactions between particles of light for advancements in photonic quantum technologies. To achieve this, a semiconductor material that mediates interactions through light-matter interactions is needed, such as cuprous-oxide (CuO_2), which possesses Rydberg exciton states [1]. Excitons are a bound state of a negatively charged electron and a positively charged "hole", that mediate strong light-matter interactions and can be engineered for applications in next-generation lasers [2] and quantum sensing [3]. By placing the material in a special optical cavity, which is a structure that traps photons of a specific wavelength within it, the light-matter interactions may be further enhanced, leading to strong-coupling and formation of polaritons [4, 5] which are an entangled quantum fluid [6, 7] of half-light/half-matter particles that carry characteristics of both photons and excitons. Polaritons can interact with each other very strongly and exhibit 'polariton blockade' [8-10]. Polariton blockade is in effect a suppression of light emission, whereby the material acts as a filter that separates a beam of laser light into a stream of single spaced photons. Cuprous oxide is a very promising candidate for realizing the blockade phenomenon using Rydberg exciton states [11]. The phenomenon of Rydberg blocakade in the solid-state has not been demonstrated, but its discovery could lead to the development of single-photon transistors, photonic quantum gates, and light-based quantum simulators.

In this work we show experimental non-resonant optical measurements of Rydberg excitonic states measured in various Cuprous Oxide samples at millikelvin temperatures and 4K temperatures. We further present preliminary data showing auto-correlation measurements in a nano-pillar etched samples. These results will pave the way for exiton-polariton measurements using fibre cavities and nanofabricated monolithic cavities, towards the ultimate goal of demonstrating the Rydberg Blockade phenomenon.

[1] T. Kazimierczuk, et al., *Nature* **514**, 343–347 (2014)
[2] C. Schneider, et al. *Nature* **497**, 348–352 (2013)
[3] C. Sturm, et al., *Nature Comms* **5**, 3278 (2014)
[4] O. El Daïfa, et al., *Appl. Phys. Lett.* **88**, 061105 (2006)
[5] B. Besga, .., T. Volz, *Phys. Rev. Applied* **3**, 014008 (2015)
[6] J. Kasprzak, et al., *Nature* **443**, 409–414 (2006)
[7] I. Carusotto and C. Ciuti, *Rev. Mod. Phys*. **85**, 299 (2013)
[8] A. Verger, C. Ciuti, and I. Carusotto *Phys. Rev. B* **73**, 193306
[9] Muñoz-Matutano,.., Volz, T. (2019). *Nature materials*, **18(3)**, 213-218.
[10] Delteil, A.,.., İmamoğlu, A. (2019). *Nature materials,* **18(3)**, 219-222.
[11] Orfanakis, K.,..,T. Volz, H. Ohadi et al. *Nat. Mater*. **21**, 767–772 (2022)

P17 Artificial bandstructure in GaAs lateral superlattices

D.Q. Wang[a], Z. Krix[a], C. Chen[b], D.A. Ritchie[b], O. Sushkov[a], A.R. Hamilton[a] and O. Klochan[a,c]

[a]*School of Physics, The University of New South Wales, Sydney, NSW, Australia.*
[b]*Semiconductor Physics Group, Cavendish Laboratory, JJ Thomson Ave, Cambridge, CB3 0HE, UK*
[c]*School of Science, The University of New South Wales, Canberra, ACT, Australia.*

The electronic properties of materials are determined by the atomic constituents and their crystal lattice structure. Engineered electronic materials, which are created by imposing a spatially periodic potential (a superlattice), have offered a powerful way to alter the properties of natural crystals in a controlled manner. For example, Moiré superlattices, where different layers of two-dimensional (2D) materials are stacked and twisted to create a superlattice potential, are currently attracting significant attention as they provide an ideal platform for both studying fundamental physics as well as promising future applications. An alternative approach to create a superlattice potential is via nanolithography techniques. It offers an excellent control of the superlattice parameters and can be easily integrated into many existing device architectures, e.g. a semiconductor FET, which has an advantage of well-established fabrication technology and superb device quality.

Using this approach, we demonstrate a versatile device architecture that allows independent control of carrier density and superlattice potential across a wide range. We detect the artificial mini bands via transport measurements of the low field Hall effect. The Hall coefficient shows multiple transitions from electron-like to hole-like behaviour as the chemical potential is swept through the different artificial bands, consistent with our band structure calculations. Furthermore, we are able to continuously tune the artificial bandstructure from free electrons to graphene-like and eventually kagome-like bands.

List of Participants

First Name	Last Name	Institution	E-mail address
Mustafa *	Abdelaal	UNSW Canberra	m.abdelaal@unsw.edu.au
Michael	Anderson	Domo-Technica	michael@domotech.com.au
Mohammed*	Asiri	University of Adelaide	mohammed.asiri@adelaide.edu.au
Matteo	Baggioli	Jiao Tong University, Shanghai	b.matteo@sjtu.edu.cn
Amanuel	Berhane	CSIRO	amanuel.michael@gmail.com
Seán	Cadogan	UNSW Canberra	s.cadogan@unsw.edu.au
Stewart	Campbell	UNSW Canberra	s.campbell@unsw.edu.au
Melissa	Carr	Ezzi Vision	mell@ezzivacuum.com.au
John	Cashion	Monash University	john.cashion@monash.edu
Oliver	Conquest	The University of Sydney	oliver.conquest@sydney.edu.au
Susan	Coppersmith	UNSW Sydney	s.coppersmith@unsw.edu.au
Dimi	Culcer	UNSW Sydney	d.culcer@unsw.edu.au
Bruno	deHarak	International Technology Centre	bruno.a.deharak.civ@army.mil
Dmitry	Efimkin	Monash University	dmitry.efimkin@monash.edu
Jack *	Engdahl	UNSW Sydney	j.engdahl@student.unsw.edu.au
Fahmida *	Fakhera	The University of Sydney	ffak3174@uni.sydney.edu.au

Trevor	Finlayson	University of Melbourne	trevorf@unimelb.edu.au
Shanice	Hew	SciTek	shanice@scitek.com.au
Chris	Howard	University of Newcastle	chris.howard@newcastle.edu.au
Wayne	Hutchison	UNSW Canberra	w.hutchison@unsw.edu.au
Taka	Kaneko	Ezzi Vision Sydney Office	taka@ezzivacuum.com.au
Masahiro *	Kawamata	Tohoku University (Japan)	masahiro.kawamata.s4@dc.tohoku.ac.jp
Naveed Aziz	Khan	Nano Vacuum Pty Ltd	naveedk@nanovactech.com
Oleh	Klochan	UNSW Canberra	o.klochan@unsw.edu.au
Zeb	Krix	UNSW Sydney	z.krix@unsw.edu.au
Krystina	Lamb	ANSTO - Australian Synchrotron	lambk@ansto.gov.au
Roger	Lewis	University of Wollongong	roger@uow.edu.au
Klaus-Dieter	Liss	University of Wollongong	kdl@uow.edu.au
Amelia	Liu	Monash University	amelia.liu@monash.edu
Kaiyu	Ma	University of Wollongong	km294@uowmail.edu.au
Andrew	Manning	ANSTO	andrewm@ansto.gov.au
Jacob	Martin	Curtin University	jacob.w.martin@curtin.edu.au
Eric	Mascot	University of Melbourne	eric.mascot@unimelb.edu.au

Daniel *	McEwen	Monash University	daniel.mcewen1@monash.edu
Oscar	Nieves	CSIRO	oscar.nieves@csiro.au
Anindya Sundar *	Paul	Macquarie University	anindyasundar.paul@hdr.mq.edu.au
Timothy	Petersen	Monash Centre for Electron Microscopy	timothy.petersen@monash.edu
Huyen	Pham	Monash University	huyen.pham@monash.edu
Ngoc Duy (David)	Pham	Halocell Energy Pty Ltd	davidp@halocell.energy
Kyle *	Portwin	University of Wollongong	kp896@uowmail.edu.au
Md Rezoanur *	Rahman	University of Wollongong	mrr263@uowmail.edu.au
Tanglaw	Roman	Flinders University	tanglaw.roman@flinders.edu.au
Kirrily	Rule	ANSTO	kirrilyr@gmail.com
Andrew	Smith	Monash University	andrewedwardsmith@gmail.com
Matthew *	Smith	Flinders University, College of Science and Engineering.	smit2052@flinders.edu.au
Tilo	Soehnel	University of Auckland	t.soehnel@auckland.ac.nz

Caleb *	Stamper	University of Wollongong	cjs901@uowmail.edu.au
Anton	Stampfl	ANSTO	aps@ansto.gov.au
Glen	Stewart	UNSW Canberra	g.stewart@unsw.edu.au
Oleg	Sushkov	UNSW Sydney	sushkov@unsw.edu.au
Oleg	Tretiakov	UNSW Sydney	o.tretiakov@unsw.edu.au
Hyma	Vallabhapurapu	Macquarie University	harish.vallabhapurapu@mq.edu.au
Feixiang	Xiang	UNSW Sydney	feixiang.xiang@unsw.edu.au
Zaiquan	Xu	Oxford Instruments Australia	Zaiquan.XU@oxinst.com
Shinichiro	Yano	NSRRC Taiwan	yano.shin@nsrrc.org.tw
Evrim	Yazgin	Royal Institution of Australia	EYazgin@riaus.org.au
Samuel	Yick	University of Auckland	samuel.yick@auckland.ac.nz
Mengyun (Molly)	You	University of Wollongong	my964@uowmail.edu.au
Dehong	Yu	ANSTO	dyu@ansto.gov.au
Mengting	Zhao	Monash University	mengting.zhao@monash.edu

Student participants are denoted by *